Developmental Biology 363 (2012) 373–387

Contents lists available at SciVerse ScienceDirect

Developmental Biology

journal homepage: www.elsevier.com/developmentalbiology

Enteric nervous system specific deletion of Foxd3 disrupts glial cell differentiation and activates compensatory enteric progenitors

Nathan A. Mundell [a,b,c], Jennifer L. Plank [a,c,d,1], Alison W. LeGrone [a,c,d], Audrey Y. Frist [a,c,d], Lei Zhu [e], Myung K. Shin [e], E. Michelle Southard-Smith [c,d,f], Patricia A. Labosky [a,b,c,d,*]

[a] Center for Stem Cell Biology, Vanderbilt University Medical Center, Nashville, TN 37232, USA
[b] Department of Pharmacology, Vanderbilt University Medical Center, Nashville, TN 37232, USA
[c] Program in Developmental Biology, Vanderbilt University Medical Center, Nashville, TN 37232, USA
[d] Department of Cell and Developmental Biology, Vanderbilt University Medical Center, Nashville, TN 37232, USA
[e] Genetically Engineered Models Department, Merck Research Laboratories, Rahway, NJ 07065, USA
[f] Department of Medicine, Vanderbilt University Medical Center, Nashville, TN 37232, USA

ARTICLE INFO

Article history:
Received for publication 22 June 2011
Revised 2 January 2012
Accepted 3 January 2012
Available online 12 January 2012

Keywords:
Neural crest
Foxd3
Enteric nervous system
Glial cells
Developmental compensation

ABSTRACT

The enteric nervous system (ENS) arises from the coordinated migration, expansion and differentiation of vagal and sacral neural crest progenitor cells. During development, vagal neural crest cells enter the foregut and migrate in a rostro-to-caudal direction, colonizing the entire gastrointestinal tract and generating the majority of the ENS. Sacral neural crest contributes to a subset of enteric ganglia in the hindgut, colonizing the colon in a caudal-to-rostral wave. During this process, enteric neural crest-derived progenitors (ENPs) self-renew and begin expressing markers of neural and glial lineages as they populate the intestine. Our earlier work demonstrated that the transcription factor Foxd3 is required early in neural crest-derived progenitors for self-renewal, multipotency and establishment of multiple neural crest-derived cells and structures including the ENS. Here, we describe Foxd3 expression within the fetal and postnatal intestine: Foxd3 was strongly expressed in ENPs as they colonize the gastrointestinal tract and was progressively restricted to enteric glial cells. Using a novel *Ednrb-iCre* transgene to delete *Foxd3* after vagal neural crest cells migrate into the midgut, we demonstrated a late temporal requirement for Foxd3 during ENS development. Lineage labeling of *Ednrb-iCre* expressing cells in *Foxd3* mutant embryos revealed a reduction of ENPs throughout the gut and loss of *Ednrb-iCre* lineage cells in the distal colon. Although mutant mice were viable, defects in patterning and distribution of ENPs were associated with reduced proliferation and severe reduction of glial cells derived from the *Ednrb-iCre* lineage. Analyses of ENS-lineage and differentiation in mutant embryos suggested activation of a compensatory population of Foxd3-positive ENPs that did not express the *Ednrb-iCre* transgene. Our findings highlight the crucial roles played by *Foxd3* during ENS development including progenitor proliferation, neural patterning, and glial differentiation and may help delineate distinct molecular programs controlling vagal versus sacral neural crest development.

Introduction

The enteric nervous system (ENS) is a large and complex network of cells that regulates motility, secretion and blood flow in the gastrointestinal (GI) tract. Within the gut muscle wall, interconnected ganglia, consisting of a diverse array of neurons and glia, are organized into the myenteric and submucosal plexi (Gershon, 2010; Gershon et al., 1993). Cells that form the ENS are derived from neural crest (NC) progenitors that arise from the dorsal neural tube at vagal and sacral levels during early embryonic development (Le Douarin and Kalcheim, 1999). The vast majority of the ENS is generated from vagal NC cells, which emigrate from the level of somites 1–7 (Le Douarin and Teillet, 1973; Yntema and Hammond, 1954). In mice, vagal NC cells enter the foregut at ~9.0 days post coitum (dpc) and migrate in a rostrocaudal wave along the entire length of the GI tract to generate both neural and glial lineages (Natarajan et al., 1999; Young et al., 1998). During this process, enteric NC-derived progenitors (ENPs) undergo extensive proliferation (Simpson et al., 2007). In the hindgut, sacral NC, originating posterior to somite 24, contributes a smaller population of ENPs that migrate in

* Corresponding author at: 9415 MRBIV, 2213 Garland Ave, Nashville, TN 37232-0494, USA. Fax: +1 615 343 2173.
E-mail addresses: nathan.mundell@vanderbilt.edu (N.A. Mundell), jennifer.l.plank@vanderbilt.edu (J.L. Plank), alison.w.legrone@vanderbilt.edu (A.W. LeGrone), audrey.frist@vanderbilt.edu (A.Y. Frist), lei_zhu@merck.com (L. Zhu), myung_shin2@merck.com (M.K. Shin), michelle.southard-smith@vanderbilt.edu (E.M. Southard-Smith), trish.labosky@vanderbilt.edu (P.A. Labosky).
[1] Present address for J.L. Plank: Laboratory of Cellular and Developmental Biology, NIDDK, NIH, Building 50, Room 3154, 50 South Drive, MSC 8028, Bethesda, MD 20892, USA.

0012-1606/$ – see front matter © 2012 Elsevier Inc. All rights reserved.
doi:10.1016/j.ydbio.2012.01.003

a caudorostral direction (Burns et al., 2000; Burns and Le Douarin, 1998). Sacral NC cells are also responsible for innervation of the urogenital system. During development, sacral NC halts migration after formation of the pelvic ganglia outside the hindgut and does not colonize the distal colon until vagal NC-derived cells are present (~13.5–14.5 dpc) (Druckenbrod and Epstein, 2005; Kapur, 2000).

Several signaling pathways converge to control cellular functions of multipotent ENPs during ENS development. Members of the GDNF family of ligands signal through Ret and its co-receptor GFRα1 to regulate the migration, proliferation, survival and neural differentiation of ENPs. The effects of GDNF/Ret signaling in ENPs are modulated, in part, by Endothelin 3 signaling mediated by Endothelin Receptor B (Ednrb). Specifically, Ednrb signaling maintains GDNF-driven proliferation (Barlow et al., 2003), and along with the transcription factor Sox10, inhibits differentiation of enteric neurons (Bondurand et al., 2006; Hearn et al., 1998; Wu et al., 1999), thus maintaining multipotent enteric neural crest stem cells (NCSCs) in an uncommitted, self-renewing state. Hirschsprung's disease, a congenital disorder characterized by failure of ENPs to completely colonize the gut resulting in absence of enteric ganglia in the colon, is directly linked to defects in NCSC function (Iwashita et al., 2003). Both humans and rodents deficient for several proteins including Sox10, and members of the GDNF and Endothelin 3 signaling pathways, suffer from aganglionosis of the distal colon and the resulting megacolon phenotype (Barlow et al., 2003; Baynash et al., 1994; Enomoto et al., 1998; Hosoda et al., 1994; Schuchardt et al., 1994; Southard-Smith et al., 1998). Because of the total loss of enteric ganglia in distal intestine of Hirschsprung's disease patients, many ENS studies have focused on this disease, however, other abnormalities of the GI tract, including chronic constipation and functional bowel disorders are likely to be caused by defects that arise during development of the ENS. NCSCs can be isolated from the ENS throughout embryogenesis and into postnatal life, and it is possible that ENS-derived NCSCs may be a source of neurons and glia for regeneration or repair of ENS disorders (Kruger et al., 2002, 2003; Metzger et al., 2009).

During ENS development, multipotent NCSCs co-exist with fate-restricted progenitors, but mechanisms coordinating proliferation and lineage specific differentiation of these separate ENP pools are not understood. Markers of neuronal differentiation are readily observed soon after ENPs invade the gut (Baetge and Gershon, 1989). In contrast, glial lineage markers are first detectable well behind the initial wavefront of migrating ENPs in the fetal mouse gut, indicating that differentiation of glia lags significantly behind differentiation of neurons (Heanue and Pachnis, 2007; Young et al., 2005). While much is known about molecules required for differentiation of enteric neurons, relatively little is understood about how enteric gliogenesis occurs. An emerging concept is that genes that initially function to maintain multipotency in NCSCs also play additional context-dependent roles in later cell fate decisions. For example, ENPs entering the foregut can be identified by Sox10 or Phox2b expression (Britsch et al., 2001; Corpening et al., 2008; Corpening et al., 2011; Kuhlbrodt et al., 1998; Natarajan et al., 1999; Young et al., 1999), both of which are individually required for formation and establishment of the ENS (Pattyn et al., 1999; Southard-Smith et al., 1998). Sox10 maintains multipotency of NCSCs by inhibiting neural cell fates (Kim et al., 2003) and its expression is downregulated in differentiating neurons but maintained in glia (Deal et al., 2006; Kim et al., 2003). Together with Notch signaling, Sox10 is required for enteric gliogenesis (Okamura and Saga, 2008; Taylor et al., 2007). Conversely, Phox2b expression levels are decreased in enteric glia (Corpening et al., 2008; Young et al., 1998) and maintained expression of Phox2b is required for developing neurons (Pattyn et al., 1999).

The forkhead transcription factor Foxd3 is one of the earliest genes expressed in NC progenitors and this expression is maintained as NC cells begin populating the GI tract (Labosky and Kaestner, 1998; Perera et al., 2006; Teng et al., 2008). Our earlier work demonstrated that a NC-specific deletion of Foxd3 in mice resulted in perinatal lethality and severe defects in most NC derivatives, including complete loss of the ENS (Mundell and Labosky, 2011; Plank et al., 2011; Teng et al., 2008). Additionally, Foxd3 is required to preserve multipotency of NCSCs and does so by repressing ectomesenchymal differentiation thereby maintaining their ability to generate neurons (Mundell and Labosky, 2011). Although Foxd3 is required for early NC development, including self-renewal and maintenance of NC multipotency, its expression and cellular functions at later stages of ENS development have not been examined.

Here, we comprehensively mapped Foxd3 expression during murine ENS development and demonstrated that Foxd3 was initially expressed in ENPs and subsequently maintained in differentiated glia. Using a novel *Ednrb-iCre* transgene, we specifically deleted *Foxd3* in a subset of vagal NC-derived ENPs to determine the functions of Foxd3 during late ENS development, after vagal NC cells colonize the proximal GI tract. Our in vivo lineage-mapping experiments demonstrated that Foxd3 functions cell-autonomously to maintain both proliferation and glial differentiation of ENPs. In addition, we discovered a sub-population of Foxd3-expressing ENPs that became activated in response to ENS defects, underwent regulative proliferation and differentiation, and compensated for initial disruption of ENS development due to loss of *Foxd3* in vagal NC-derived cells.

Materials and methods

Mouse lines

Foxd3 alleles were described previously (Hanna et al., 2002; Teng et al., 2008). The *Foxd3* null allele $Foxd3^{tm2.Lby}$ harboring a GFP reporter (called $Foxd3^{GFP}$) was used for some expression analyses, while an alternative null allele, $Foxd3^{tm1.Lby}$, (called $Foxd3^{-}$ throughout) was used in combination with $Foxd3^{tm3.Lby}$, the *Foxd3* conditional allele (called $Foxd3^{flox}$), for tissue-specific deletion. The *Ednrb-iCre* transgenic line was generated by standard microinjection techniques (Nagy et al., 2003). Mouse lines were interbred to generate $Foxd3^{flox/-}$; *Ednrb-iCre* (mutant) and $Foxd3^{flox/+}$; *Ednrb-iCre* (littermate control) embryos or mice. For lineage analyses, mice carrying Cre reporter alleles *Gt(ROSA)26Sor*^{tm1Sor} (called $R26R^{lacZ}$) or *Gt(ROSA)26Sor*$^{tm1(EYFP)Cos}$ (called $R26R^{YFP}$) were incorporated into the crosses (Soriano, 1999; Srinivas et al., 2001). In some experiments, the *Wnt1-Cre* transgenic line (Danielian et al., 1998) was used to lineage-map NC. All lines were on a mixed genetic background (CD-1, 129S6, and C57BL/6) and maintained in accordance with protocols approved by the Vanderbilt University Institutional Animal Care and Use Committee (IACUC). DNA for genotyping was extracted from embryonic yolk sac or tail biopsies, and the presence of the *Ednrb-iCre* transgene was detected by genotyping for *iCre* with primers (*5′-GACAGGCAGGCCTTCTCTGAA-3′*) and (*5′-CTTCTCCACACCAGCTGTGGA-3′*) that amplify a 522 bp fragment. The PCR conditions were 30 cycles of 94 °C, 58 °C, and 72 °C, each for 45 s, followed by 72 °C for 10 min. Genotyping for *Foxd3* alleles was as described (Hanna et al., 2002; Teng et al., 2008).

Embryonic dissections and enteric muscle strip preparations

For timed pregnancies, females were checked daily for the presence of a vaginal plug, and noon on the day of plug designated 0.5 days post coitum (dpc). GI tracts (esophagus to anus) were dissected from 10.5 to 16.5 dpc embryos in ice cold PBS, mesentery and other associated organs were removed, and tissue fixed in 4% paraformaldehyde (PFA) in phosphate buffered saline (PBS) for 4 h or overnight and washed in PBS. For muscle strips, the GI tract was dissected from postnatal (P11–P14) or adult mice (2–3 months old) and fixed for 6–8 min in ice-cold neutral buffered formalin. After initial fixation, the intestine was further dissected into three segments corresponding to the duodenum and the proximal and distal halves of the colon. The inner and outer muscle layers, containing the

myenteric plexus, were separated from the submucosa of the gut and fixed in 4% PFA for 4 h on ice.

Histology and immunohistochemistry

For wholemount immunohistochemistry, samples were processed as described previously (Corpening et al., 2011). Briefly, tissues were fixed as described above, permeabilized in 0.5% Triton X-100 at room temperature for 30 min and blocked for 4 h or overnight at 4 °C in 10% normal donkey serum, 0.1% Triton X-100 with or without 1% BSA in PBS. After blocking, tissue was incubated in primary antibodies at dilutions given below, washed in PBS with 0.1% Triton X-100, incubated with secondary antibodies and washed, with each step performed overnight at 4 °C. For imaging, GI tracts and muscle strips were positioned flat on glass slides and cover-slipped with Aqua Poly-Mount (PolySciences). For immunohistochemistry on paraffin sections, 10.5 dpc embryos were fixed in 4% PFA in PBS overnight, and processing and histology performed using standard procedures (Presnell and Schreibman, 1997). The following primary antibodies were used: chicken anti-GFP to detect green fluorescent protein (GFP) from the *Foxd3*^{GFP} allele and also for yellow fluorescent protein (YFP) expression from the Cre-recombined and activated *R26R*^{YFP} allele (used at 1:500, Abcam), rabbit anti-phospho-histone H3 (pH3) (1:200, Upstate Biotechnology), mouse anti-β-III tubulin (TUJ1) (1:500, Covance), mouse anti-glial fibrillary acidic protein (GFAP) (1:500, Sigma), rabbit anti-Foxd3 (1:500, (Tompers et al., 2005), rabbit anti-fatty acid binding protein 7 (FABP7) (1:500, gift from Dr. Thomas Muller (Young et al., 2003)), rabbit anti-p75 (1:200, Promega), rabbit anti-protein gene product 9.5 (PGP9.5) (1:1000, AbD Serotec), rabbit anti-S100b (1:500, Dako), and goat anti-Sox10 (1:15 or 1:20, Santa Cruz). Secondary antisera were purchased from Jackson ImmunoResearch: Cy2 donkey anti-chicken (1:500), DyLight™ 488 donkey anti-chicken (1:500), Cy3 donkey anti-mouse (1:700), Cy3 donkey anti-rabbit (1:700), Cy3 donkey anti-goat (1:700), Cy5 donkey anti-mouse (1:500), Cy5 donkey anti-rabbit (1:500), Cy5 donkey anti-goat (1:500). 4,6-diamidino-2-phenylindole, dihydrochloride (DAPI, 1:5000, Molecular Probes) was used to detect nuclei. Immunohistochemical experiments were imaged using either an Olympus FV1000 laser scanning confocal microscope or a Zeiss Axio Observer A1 fluorescence microscope and AxioCam MRc5 camera. 5-bromo-4-chloro-3-indolyl-β-D-galactoside (X-gal) reactions (Nagy et al., 2003) and wholemount acetylcholinesterase (AChE) enzyme histochemistry (Cantrell et al., 2004; Enomoto et al., 1998) were performed as described and imaged with a Nikon SMZ-U stereomicroscope and Q-Imaging Micropublisher camera. Whole mount preparations were imaged on a Leica MZ 16 FA stereoscope with a QImaging RETIGA 4000R camera.

Quantification of enteric cell types

To quantify enteric cell type specific markers and proliferation in cells with Ednrb-iCre activity, GI tracts from 12.5 dpc–16.5 dpc *Ednrb-iCre; R26R*^{YFP} fate-mapped embryos were isolated, subjected to immunofluorescence for YFP, p75, PGP9.5, Foxd3, Sox10 and/or pH3 as indicated, and stained with DAPI as described above. Confocal images of non-overlapping fields were captured with a 40× objective, corresponding to ~0.1 mm^2 per field (x, y) with optical thicknesses (z) ranging from 0.8 to 1.6 μm, with the thickness consistent within each experiment. The z-dimension image from each field that contained the highest number of YFP-expressing cells, and was therefore presumably focused on the myenteric plexus, was digitally analyzed using MetaMorph™ software to determine the total number of YFP, p75, PGP9.5, Foxd3, Sox10, DAPI and/or pH3-positive cells as indicated in individual experiments. Three random fields were quantified in the duodenum and in embryos 14.5 dpc or older, six semi-contiguous fields were also scored in the distal colon from each sample. To determine densities of PGP9.5-expressing cells in colons from control and mutant embryos single confocal z-dimension images from six distinct regions of the colon were thresholded equally and digitally analyzed for area of PGP9.5 and DAPI-positive pixels using ImageJ software (Abramoff et al., 2004). To quantify enteric glia in adult gut muscle strips, the total number of S100b-positive cells and S100b and YFP-expressing glia were counted in four-five random 20× fields of the duodenum from three control and five mutant animals and the distal half of the colon from three control and four mutant mice. Images were quantified blindly by two observers using Photoshop software to compare YFP and S100b signals in individual and merged channels and are presented as the average percent of S100b-positive cells that co-expressed YFP. Statistics were calculated as mean ± standard error of the mean (SEM) and significance determined with a two-tailed Student's *t*-test.

Results

Foxd3 is expressed in ENPs and progressively restricted to glia during ENS development

During early NC development (8.0–10.5 dpc), Foxd3 is initially expressed in all NC cells, but expression is extinguished in cranial and cardiac NC prior to their differentiation into mesenchymal lineages (Labosky and Kaestner, 1998; Mundell and Labosky, 2011; Perera et al., 2006). Although Foxd3 expression has been reported in the ENS at 10.5–13.5 dpc (Labosky and Kaestner, 1998; Perera et al., 2006; Teng et al., 2008), expression during ENS development had not been investigated in detail or characterized with cell-type specific markers. Therefore, we examined Foxd3 expression in *Wnt1-Cre; R26R*^{YFP} lineage-traced ENPs after their initial colonization of the foregut. At 10.5 dpc, Foxd3 protein expression is detected in the nucleus of YFP-positive cells in the proximal GI tract (Fig. 1A–A″), consistent with its expression in nearly all ENPs at early stages of ENS development. To circumvent difficulties inherent with antibodies generated from the same species and to label Foxd3-expressing cells throughout the cytoplasm, we examined immunohistochemical co-localization of Foxd3 with GFP from the *Foxd3*^{GFP} allele using cell-type specific markers, an approach used previously (Perera et al., 2006). To confirm that GFP from the *Foxd3*^{GFP} allele accurately represented endogenous Foxd3 expression, we examined GFP and Foxd3 protein expression during late ENS development in 16.5 dpc *Foxd3*^{GFP} embryos and in gut muscle strips from postnatal day 14 (P14) *Foxd3*^{GFP} mice. At both stages, Foxd3 protein was co-expressed in the nuclei of GFP-positive cells throughout the ENS in the majority of cells (Fig. 1B–C″), indicating that Foxd3 was expressed in ENPs during and after enteric neuron and glial lineage segregation. We detected very few GFP-positive cells that lacked staining for Foxd3 protein (Fig. 1B–B″, green arrows), which may result from the perdurance of GFP or examination of focal planes lacking a nucleus.

To establish the identity of Foxd3-expressing cells within enteric ganglia we performed immunohistochemical co-localization of GFP with markers for undifferentiated NC cells, neurons and glia. Consistent with a role for Foxd3 in enteric neural/glial progenitors, at 16.5 dpc, GFP expression largely overlapped with expression of the low-affinity nerve growth factor receptor (p75), a NC progenitor and ENP marker (Fig. 2A–A″). In addition to GFP/p75 double-positive cells, we detected a small population of GFP-positive cells that did not express p75 (green arrows), suggesting that these cells may have initiated differentiation (Fig. 2A). To assess the differentiation status of Foxd3-expressing cells, we examined GFP expression together with expression of the neural marker PGP9.5. At 16.5 dpc, most Foxd3-expressing cells were located adjacent to neurons and very few GFP-positive cells co-expressed PGP9.5 (yellow arrow in Fig. 2B), indicating that Foxd3 was not expressed in differentiating neurons. Further analysis of postnatal enteric ganglia confirmed absence of Foxd3 expression in neurons but showed Foxd3 expression

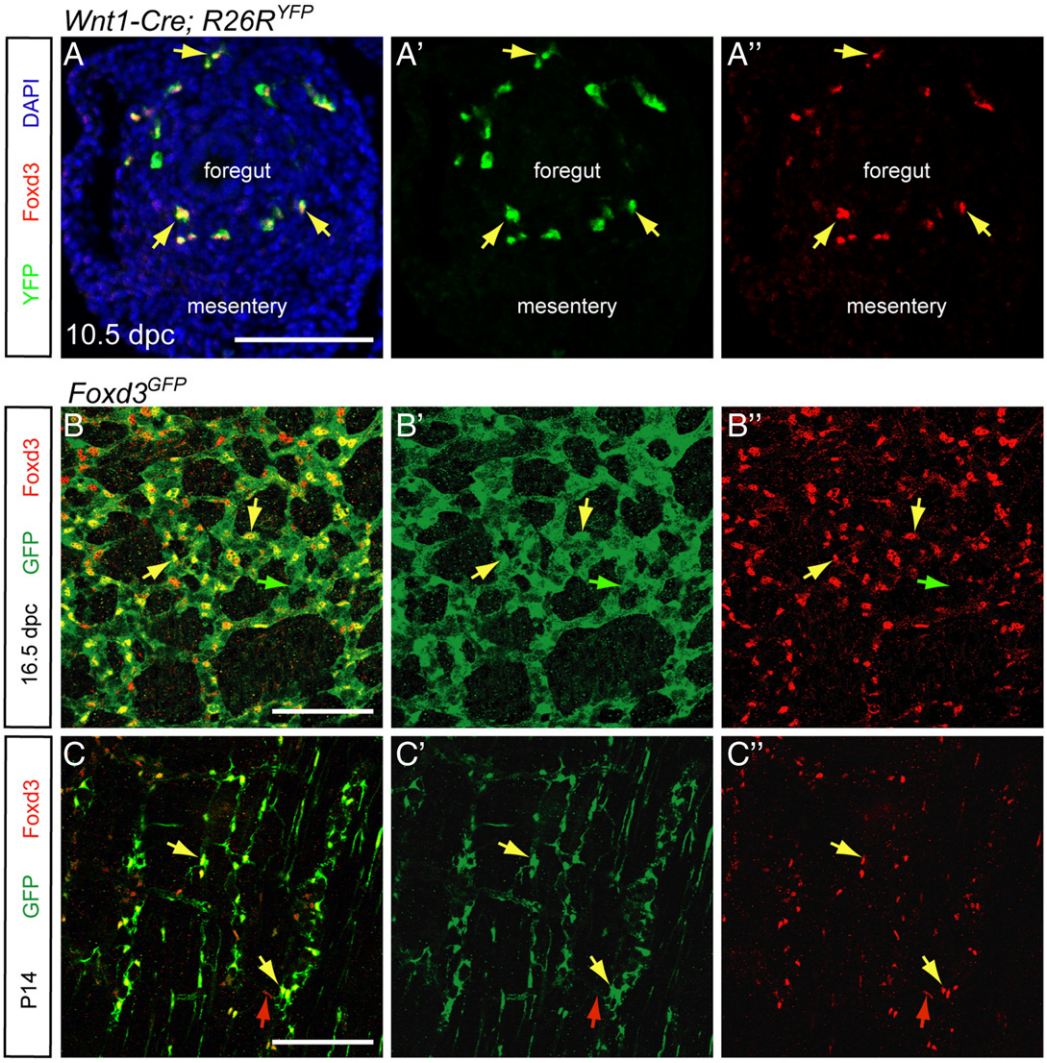

Fig. 1. Foxd3 is expressed throughout ENS development.(A) Transverse sections through the proximal foregut of a *Wnt1-Cre; R26R*^{YFP} (NC fate-mapped) embryo showed co-labeling of YFP (green) and Foxd3 (red) expression at 10.5 dpc (A–A″, yellow arrows). (B–C) Confocal images of wholemount 16.5 dpc GI tract (B–B″) and postnatal day 14 gut muscle strips from the duodenum (C–C″) of *Foxd3*^{GFP} embryos and mice showed expression of GFP from the *Foxd3*^{GFP} allele (green) filling the cytoplasm and nuclei of cells with Foxd3 protein (red) in the nuclei. At both stages, Foxd3 protein expression overlapped with GFP expression (yellow arrows), with only a few cells that expressed only GFP (green arrow, B) or Foxd3 protein (red arrows). Images in B–C″ were captured with a 40× oil objective. Scale bars = 100 μm.

in cells closely associated with PGP9.5-positive cells (Fig. 2C). Images of individual channels for Fig. 2A–C are in Fig. S1.

The smaller stellate morphology and location of Foxd3-expressing cells closely juxtaposed to enteric neurons strongly suggested that these cells were enteric glia. To address this possibility, we performed co-immunodetection of the glial cell markers Sox10 and S100b with GFP from the *Foxd3*^{GFP} allele at embryonic and postnatal stages. At 16.5 dpc, nearly all NCSCs and glia, marked by Sox10, were co-labeled with GFP (Fig. 2D), demonstrating that Foxd3 is maintained in ENPs and glia. By P14, co-localization of GFP and Sox10 indicated that Foxd3 expression is maintained in mature enteric glial cells (Fig. 2E). Further immunofluorescent co-labeling of GFP and the mature glial marker S100b also showed almost complete overlap with GFP expression from the *Foxd3*^{GFP} allele at 16.5 dpc and P14 (Fig. 2F, G). Individual channel images for Fig. 2D–G are in Fig. S2. Immunodetection with FABP7, a marker of immature and mature glia, and TUJ1, a neuronal marker, revealed a similar pattern of co-expression with Foxd3 in glia but not neurons (Fig. S3 A–B‴). Together, these expression patterns demonstrated that Foxd3 was broadly expressed in ENPs, progressively downregulated as cells underwent neuronal differentiation, and maintained in differentiated glia.

Spatiotemporal characterization of Ednrb-iCre activity

Previous tissue-specific deletion of *Foxd3* within early, and presumably uncommitted, NC progenitors with *Wnt1-Cre* or *Pax3*^{Cre} resulted in a complete loss of the ENS (Mundell and Labosky, 2011; Nelms et al., 2011; Plank et al., 2011; Teng et al., 2008). However, it is not known whether Foxd3 is required later in the sublineage of NC cells that generate enteric neurons and/or glia. To conditionally delete *Foxd3* after specification of ENPs and initial migration of vagal NC cells into the GI tract, we generated a transgenic mouse line, *Ednrb-iCre*, in which expression of Cre-recombinase is directed by an ENS-specific enhancer of *Ednrb* (Fig. 3A). This *Ednrb* enhancer was characterized previously and consists of a genomic fragment (−1.2 kb to −160 bp) upstream of the *Ednrb* start site (Zhu et al., 2004). This ~1 kb enhancer in combination with a minimal promoter is sufficient to direct expression to ENPs after they colonize the foregut and small intestine. To generate these transgenic mice, the enhancer element was linked to an *Hspa1b* (*Hsp68*) minimal promoter to direct expression of a codon-improved Cre recombinase (iCre) (Shimshek et al., 2002). The tissue specificity of Cre activity from this transgene was verified by breeding *Ednrb-iCre* mice with *R26R*^{lacZ} or *R26R*^{YFP} reporter mice in which Cre expression results in

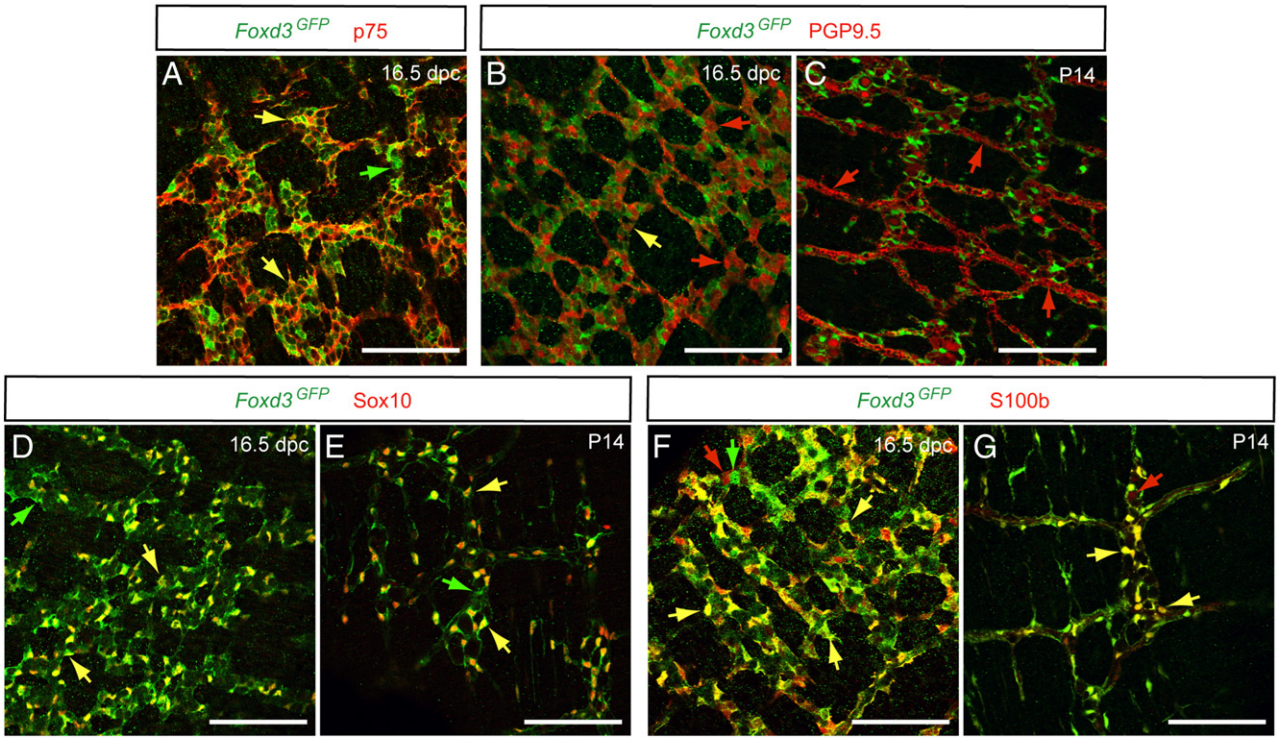

Fig. 2. Foxd3 is expressed in ENPs and glia during ENS development, but downregulated in the majority of enteric neurons. (A) Immunofluorescent detection of GFP from the *Foxd3*^{GFP} allele (green) together with p75 (red) revealed expression of Foxd3 in ENPs in the duodenum from 16.5 dpc embryos (A, yellow arrows) and in a smaller subset of cells that did not express p75 (green arrow). (B–C) GFP expression in combination with PGP9.5 (red) demonstrated that Foxd3 protein was largely absent from most PGP9.5-expressing enteric neurons in the duodenum at 16.5 dpc (B). Yellow arrows identify a small population of cells that co-expressed GFP and PGP9.5 and red arrows indicate cells that expressed only PGP9.5. In postnatal gut muscle strips Foxd3 was expressed in cells adjacent to neurons, but was not detected in the majority of PGP9.5-expressing neurons (C, red arrows). (D–G) GFP was extensively co-localized with Sox10 (red) in glial cells in 16.5 dpc GI tracts (D) and in postnatal gut muscle strips (E). Yellow arrows indicate cells that co-expressed GFP and Sox10. 16.5 dpc GI tracts from *Foxd3*^{GFP} embryos (F) and gut muscle strips from *Foxd3*^{GFP} postnatal day 14 mice (G) processed with antibodies against GFP (green) and S100b (red) confirmed Foxd3 expression in glial cells during specification of enteric lineages. Examples of cells that co-expressed GFP and S100b are indicated with yellow arrows. Red arrows indicate S100b-positive cells that lacked GFP expression and green arrows indicate cells that expressed GFP but not S100b. Images were captured with a 40× oil objective. Scale bars = 100 μm.

excision of a stop codon and expression of *lacZ* or YFP. In wholemount analysis of *Ednrb-iCre; R26R*^{lacZ} embryos, X-gal staining was faintly detected in the developing GI tract when ENPs are approaching the cecum at 11.0 dpc (40–42 somite stages), but was not detected in embryos 10.5 dpc or younger (Fig. 3B–C′). Later, at 11.5 dpc, Cre activity was detected in ENPs populating the GI tract from the esophagus to the cecum (Fig. 3D–E′). Cre activity was also detected within the neural tube (Fig. 3F–G) as expected (Lee et al., 2003; Zhu et al., 2004); however, activity within the NC was limited to ENPs within the GI tract and was not detected in other NC derivatives including NC in the outflow tract of the heart, skin, cranial ganglia or dorsal root ganglia (DRG) (Fig. 3C–G and data not shown).

Ednrb-iCre activity is specific to vagal NC-derived cells

To determine if Foxd3 is expressed in cells with *Ednrb-iCre* mediated Cre activity, we evaluated Foxd3 protein expression in the duodenum versus colon from *Ednrb-iCre; R26R*^{YFP} lineage-traced embryos. At 15.5 dpc, the vast majority of Foxd3-expressing cells in the duodenum showed *Ednrb*-iCre-activated YFP expression (Fig. 4A) indicating Cre activity in ENPs and differentiating glia. This pattern was identical to previously reported co-expression of this enhancer with Sox10 in vagal NC-derived progenitor cells (Zhu et al., 2004). Examination of Foxd3 and YFP expression at higher magnification revealed that a small fraction of Foxd3-expressing cells did not exhibit Cre activity (red arrow, Fig. 4A′), suggesting that a small sub-population of Foxd3-expressing ENPs did not activate the *Ednrb* enhancer. At this stage, sacral NC-derived ENPs are present in the distal colon and in the adjacent pelvic ganglia. *Ednrb* is expressed in sacral NC (Delalande et al., 2008), however, it was unknown whether the 1 kb enhancer region drives expression in both vagal and sacral ENPs. Analysis of YFP and Foxd3 expression in lineage mapped embryonic colons revealed two distinct populations of Foxd3-expressing cells: a population co-expressing both Foxd3 and YFP (yellow arrows, Fig. 4B–B′), and a smaller population of Foxd3-positive cells lacking Cre activity (red arrows, Fig. 4B–B′). To address the question of whether the transgene was expressed in all p75-expressing ENPs, we again used wholemount immunofluorescence in lineage mapped embryos and showed that the Cre-activated YFP from the *R26R*^{YFP} allele was co-localized with p75 in the majority of ENPs at 12.5 dpc and at 15.5 dpc (yellow arrows in Fig. 4C, D). Quantification of these data revealed that in 12.5 dpc embryos, the majority of p75-expressing cells also expressed YFP (~95%, red arrow, Fig. 4C, quantification in Fig. 4E) and this population decreased to approximately 80–82% at 15.5 dpc (Fig. 4D, E). We used the same approach to determine whether the *Ednrb-iCre* lineage included enteric neurons using immunohistochemistry for YFP together with PGP9.5 at 12.5 dpc and 15.5 dpc (Fig. 4F, G). These data showed that the lineage-mapped neural population does not overlap as completely compared to the p75 population; approximately 53–62% of PGP9.5-positive enteric neurons are labeled by this transgene at both stages. These data are quantified in Fig. 4H.

The decreased overlap of Foxd3 and YFP expression observed in the colon versus the duodenum (Fig. 4) suggests two non-exclusive possibilities: 1) that *Ednrb-iCre* activity is specific to vagal ENPs and is not present in sacral ENPs, or 2), that a significant number of Foxd3-expressing cells do not express Cre and/or have delayed activation of the transgene. To determine if Cre activity was present in sacral NC derivatives, we examined expression of p75 in the sacral NC-derived pelvic plexus and compared this to activation of the *R26R*^{YFP} reporter with the NC-specific *Wnt1-Cre* transgene versus *Ednrb-iCre*. At 14.5 dpc,

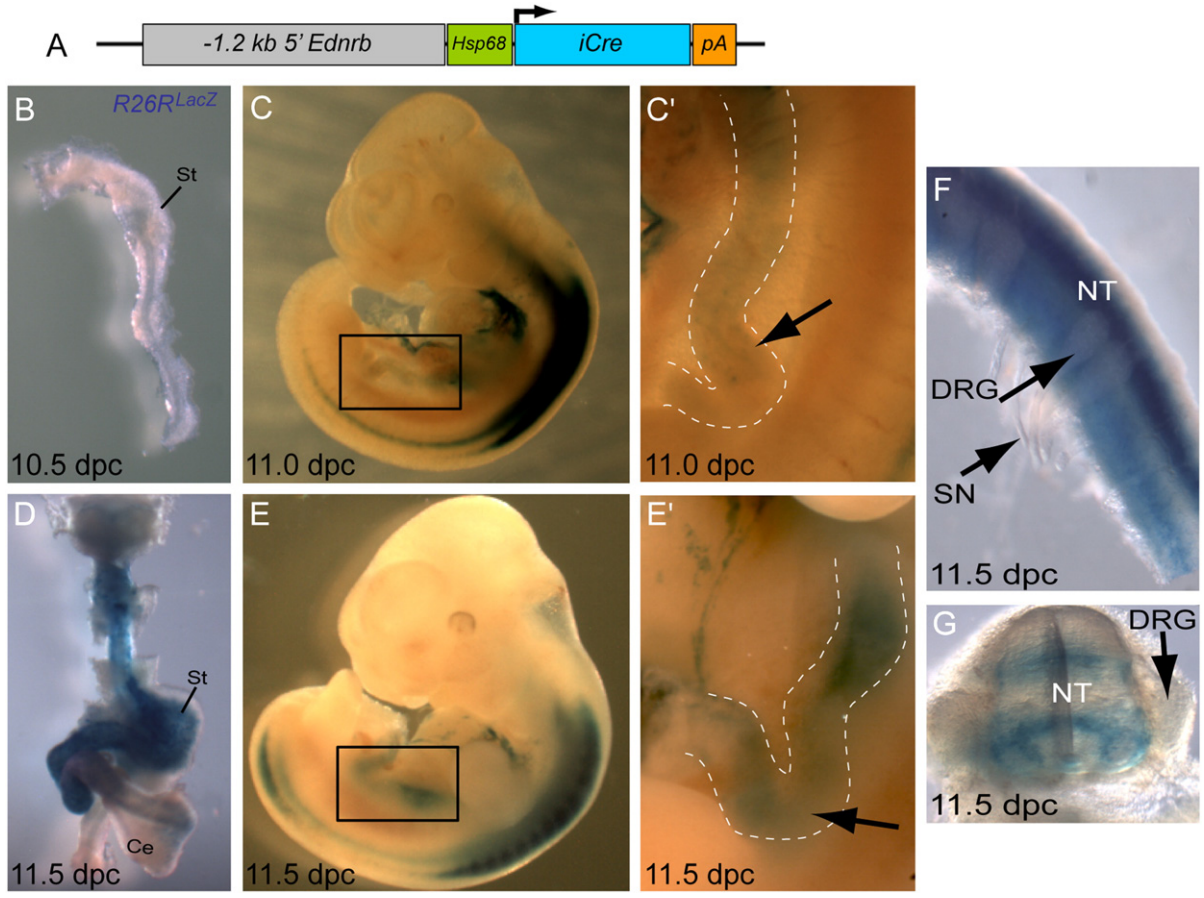

Fig. 3. Temporal activity of Cre-recombinase in *Ednrb-iCre; R26R*^{lacZ} embryos during ENS development. (A) Diagram of the construct used to generate *Ednrb-iCre* transgenic mice. (B–E′) All samples were stained for beta-galactosidase activity from the recombined *R26R*^{lacZ} allele (blue). At 10.5 dpc, X-gal-positive cells were not detected in the GI tract from *Ednrb-iCre; R26R*^{LacZ} embryos (B). Beginning at 11.0 dpc (40–42 somite stages), X-gal-positive cells were detected in the neural tube and faint beta galactosidase activity was observed in ENPs (C, C′, arrow). At 11.5 dpc, *Ednrb-iCre* was strongly activated and Cre activity detected in ENPs throughout the GI tract to the level of the cecum (D, E, E′). In B and D the dissected GI tracts are shown with the rostral end at the top of the panel. Boxes in C and E show fields for C′ and E′ turned 90° counterclockwise. (F, G) Sub-dissection of neural tube and DRG from an 11.5 dpc embryo showed X-gal-positive cells detected in distinct domains in the neural tube. X-gal-positive cells were not detected in DRG (F, G). G is a transverse view of the neural tube shown in F. Abbreviations: Ce, cecum; DRG, dorsal root ganglion; Hsp68, heat shock protein 68 minimal promoter; NT, neural tube; pA, polyadenylation tail; SN, spinal nerves; St, stomach.

Wnt1-Cre fate-mapped YFP-expressing sacral NC-derived cells were present within pelvic ganglia as marked by p75 (pelvic ganglion indicated by arrows, Fig. 5A–A′). In stark contrast, *Ednrb-iCre* mediated expression of YFP was not detected in pelvic ganglia at 14.5 dpc or 16.5 dpc (Fig. 5B–E′), although YFP-expressing cells are detected within the colon in the same samples. These data suggest that *Ednrb-iCre* expression is limited to vagal NC-derived ENPs, and highlight the utility of this Cre transgene to label and distinguish vagal ENPs versus those derived from the sacral NC.

Effect of deleting Foxd3 in ENPs using Ednrb-iCre

Foxd3 is required for NC colonization of the GI tract and establishment of all ENPs (Teng et al., 2008), but its role in later ENS development had not been explored. To selectively delete *Foxd3* within the vagal NC-derived ENS, we mated *Foxd3*$^{flox/flox}$ and *Foxd3*$^{+/-}$; *Ednrb-iCre* mice to obtain *Foxd3*$^{flox/+}$; *Ednrb-iCre* (control) and *Foxd3*$^{flox/-}$; *Ednrb-iCre* (mutant) mice (matings diagrammed in Fig. 6). Embryos and mice were found in expected ratios for each genotype at all stages during development and as adults, suggesting that no lethality was caused by loss of *Foxd3* in the *Ednrb-iCre* lineage. Litters were monitored for general health and appearance and GI tracts dissected to determine whether these mice suffered from megacolon phenotypes. However, *Foxd3* mutant mice survived well into adulthood with overtly normal morphology of the entire GI tract. There were no differences in weight of control and mutant littermates (data not shown) suggesting little or no defects in nutrition, overall growth and general health of mutant mice.

To determine if enteric neurons were disrupted in postnatal (P11) or adult (6 week old) mice we performed wholemount analysis of enteric neurons labeled by acetylcholinesterase (AChE) activity. As expected from the health of the animals, neurons were present in enteric ganglia throughout the GI tracts from control and mutant mice although the patterning of duodenal ganglia appeared slightly irregular with greater spaces between ganglia (Fig. 7A, B). To better understand this result and verify that Foxd3 was absent in Cre-expressing cells, we used wholemount immunodetection of Foxd3 and YFP in isolated GI tracts from 16.5 dpc embryos carrying the *R26R*^{YFP} reporter allele. In control embryos, the majority of Foxd3-expressing cells in both the duodenum and colon showed co-labeling with Foxd3 and YFP (yellow arrows, Fig. 7C, D), though a population of Foxd3-expressing cells did not show Cre activity (red arrows, Fig. 7C, D). In contrast, in *Foxd3* mutant embryos, we detected a large number of Foxd3-positive ENS cells that did not express Cre (red arrows in Fig. 7C–D). Despite the reduced number of YFP-expressing cells in GI tracts from mutant embryos, the overall number of Foxd3-expressing cells was similar between control and mutants in both the duodenum and colon (Fig. 7C, D; individual channels shown in Fig. S4; data quantified in Fig. 7E–F). The large number of Foxd3-expressing cells in mutants was not due to a failure of Cre to delete *Foxd3* in the *Ednrb-iCre* lineage; Foxd3 expression was not detected in YFP-expressing cells in the duodenum and only a few cells showed co-labeling in the colon (yellow arrow, Fig. 7D), indicating efficient

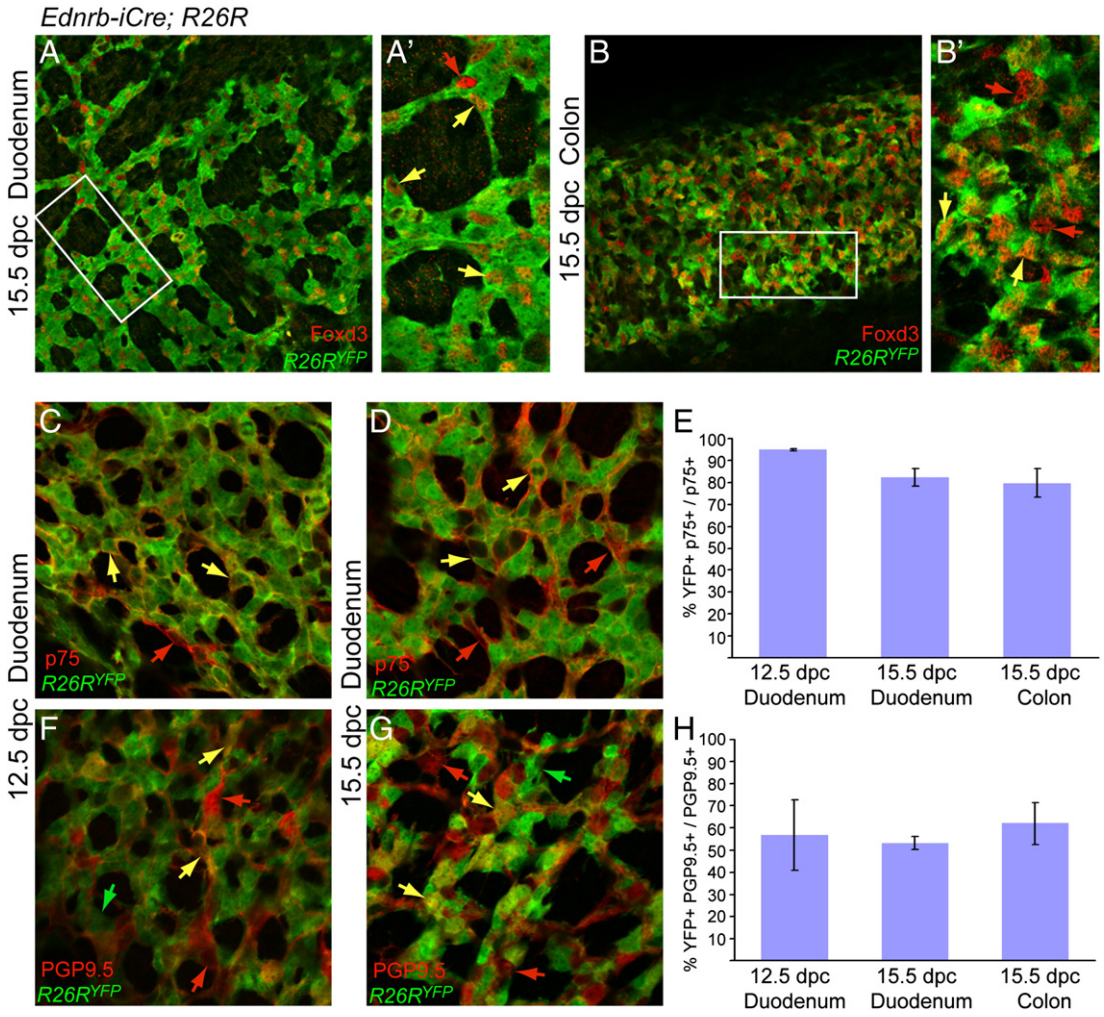

Fig. 4. *Ednrb-iCre* activity labels the vast majority of ENS progenitors during development. (A–B) Wholemount immunofluorescence at 15.5 dpc revealed that Foxd3 expression (red) in the duodenum overlapped extensively with *Ednrb-iCre* mediated YFP expression (green) from the $R26R^{YFP}$ allele (yellow arrows in A, A′). Overlap of Foxd3 and YFP expression was reduced in the colon (B, B′) compared to the duodenum (A, A′) indicating increased numbers of Foxd3-expressing cells lacking *Ednrb-iCre* activity (red arrows A′, B′). Boxes in A and B indicate the fields shown in A′ and B′, reoriented as shown. (C–E) Wholemount immunodetection revealed that YFP was extensively co-localized with p75 (red) in ENPs at 12.5 dpc (C) and at 15.5 dpc (D). Yellow arrows in C and D indicate the majority population of ENPs that co-expressed YFP and p75. A small population (~5%) of p75+ cells did not show *Ednrb-iCre* activity in GI tracts from 12.5 dpc embryos (red arrows, C, D) and this population increased in number to ~18–20% at 15.5 dpc (quantified in E). (F–H) Immunohistochemistry for YFP and the neural marker PGP9.5 (red) at 12.5 dpc (F) and 15.5 dpc indicated that Ednrb-iCre activity labels enteric neurons at both early and late stages of ENS development. Quantification of PGP9.5-expressing cells is shown in H. Data in E and H represent p75 or PGP9.5-positive cells imaged with a 40× oil objective and counted in random fields of duodena from 12.5 dpc embryos or duodena and colons from 15.5 dpc embryos (n = 3 for each). All statistics are mean ± SEM, *($p<0.05$).

deletion of the $Foxd3^{flox}$ allele by *Ednrb-iCre*. These curious results suggested a cell-autonomous role for Foxd3 during ENS development (as indicated by reduced numbers of YFP-positive cells) but also implied that a sub-population of Foxd3-expresssing ENPs that does not express *Ednrb-iCre* may expand and compensate for the apparent reduction in *Ednrb-iCre* lineage cells.

Foxd3 is required to maintain ENPs during development

Although our initial analysis of *Foxd3* mutant mice suggested that they had an overtly functional ENS, slight patterning irregularities observed in enteric ganglia (Fig. 7A–B) and the prominent role of Foxd3 in early NC development prompted us to focus our analysis on earlier developmental stages. To determine if Foxd3 is required for proper migration, distribution, and patterning of vagal NC-derived ENPs, we evaluated GI tracts from control and mutant embryos with *Ednrb-iCre* activated $R26R^{lacZ}$ and X-gal staining from 11.5 dpc to 15.5 dpc. After initial expression of Cre at 11.5 dpc in $Foxd3^{flox/+}$; *Ednrb-iCre* (control) embryos, many X-gal-positive cells were detected on the surface of the proximal GI tract up to the level of the cecum-hindgut boundary, consistent with their identity as ENPs (Fig. 8A, inset). In $Foxd3^{flox/-}$; *Ednrb-iCre* (mutant) embryos at 11.5 dpc, X-gal staining was initially modestly reduced and X-gal-positive cells were detected at caudal levels in the cecum similar to controls (Fig. 8B). In contrast, direct comparison of X-gal labeling in *Foxd3* mutant and littermate controls at 13.5 dpc demonstrated a pronounced decrease in the density of ENPs in the GI tract from mutant embryos compared to controls (Fig. 8C, D). Control vagal NC-derived ENPs had migrated through the proximal half of the hindgut at 13.5 dpc (Fig. 8C). Despite their decreased numbers, *Foxd3* mutant cells migrated to a comparable level in the colon (Fig. 8C, D). By 15.5 dpc, when control vagal NC cells had completed colonization of the GI tract to the distal end of the colon (Fig. 8E, E′), the number of mutant X-gal labeled cells was severely reduced throughout the gut (Fig. 8F) and no Xgal-positive cells were detected in the distal colon from 15.5 to 16.5 dpc embryos (arrow in Fig. 8F′ and data not shown). Using the $R26R^{YFP}$ reporter allele to facilitate visualization of sparse Cre-expressing cells, we again detected decreased numbers of mutant YFP-positive cells in the distal tip of the colon at 16.5 dpc (Fig. 8G–H). These data demonstrated a progressive reduction of

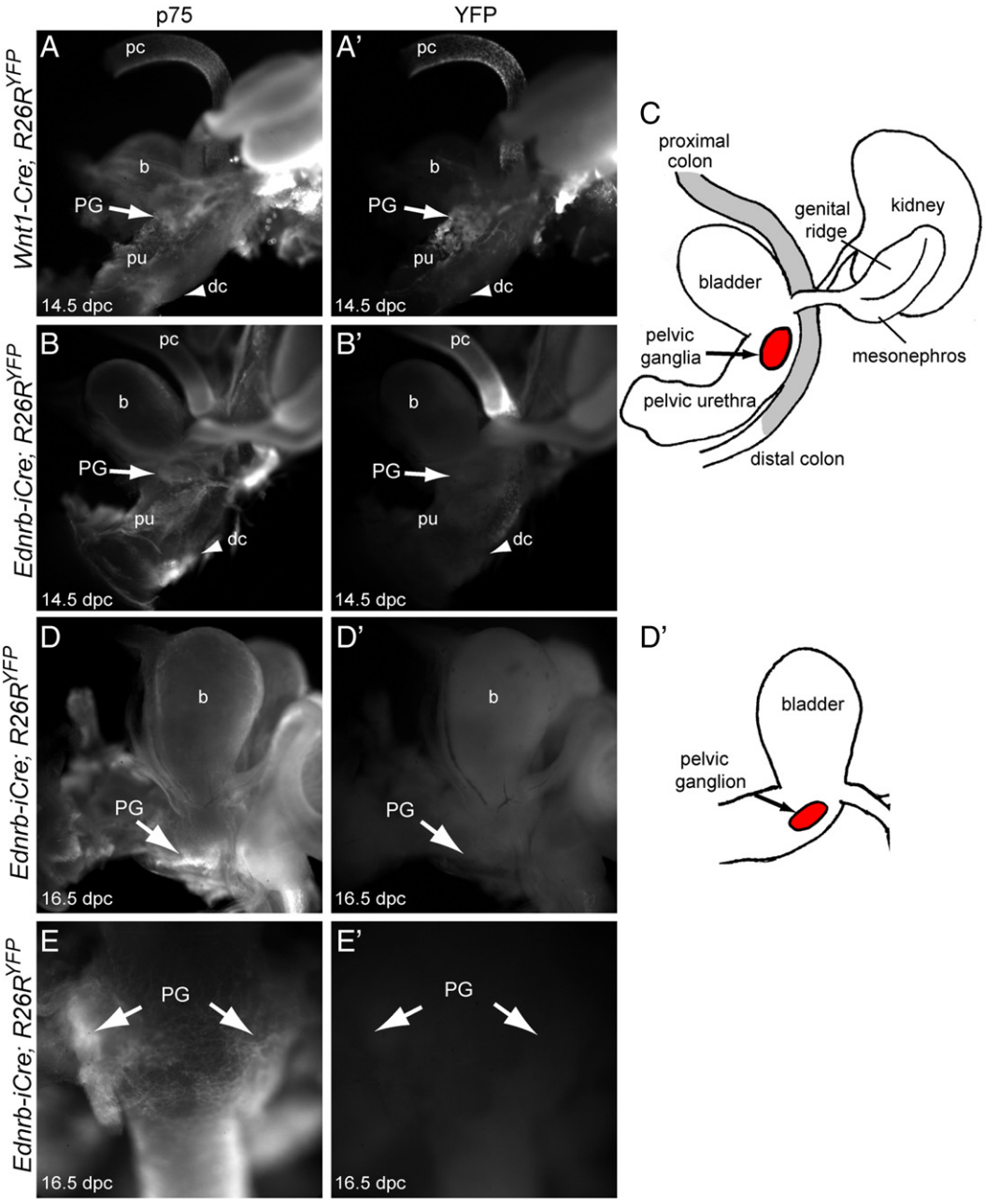

Fig. 5. *Ednrb-iCre* is active in vagal NC but not sacral NC during ENS development. (A-A′) Wholemount immunohistochemistry of a 14.5 dpc colon and lower urogenital tract for p75 (A) and *Wnt1-Cre* mediated YFP expression from *R26R*^{YFP} (A′) identified NC-derived cells in both the proximal colon and pelvic ganglion (arrow). (B–B′) In *Ednrb-iCre; R26R*^{YFP} embryos, p75 expression labeled sacral NC cells within the pelvic ganglion (arrow in B). *Ednrb-iCre* mediated YFP expression was not detected in p75-positive sacral NC cells in the pelvic ganglion (arrow in B′) but was present in vagal NC-derived cells in the colon (B′). (C). Drawing illustrates orientation of the GI and urogenital tracts shown in A–B′; this is a lateral view of the organs as viewed from the left side. Red oval indicates location of sacral NC-derived cells in the pelvic ganglion and gray shading indicates vagal NC present in the colon. This pattern is maintained at 16.5 dpc (D–E′). Wholemount immunohistochemistry of a urogenital tract from a *Ednrb-iCre* fate-mapped 16.5 dpc embryo (D–D′) shows p75 expressing sacral NC cells within the pelvic ganglion (D) that do not have *Ednrb-iCre* mediated YFP expression from *R26R*^{YFP} (D′). Cartoon in D″ illustrates lateral orientation of the urogenital tract shown in D–D′; red oval indicates location of sacral NC-derived cells in the pelvic ganglion. Images in E–E′ show p75 expression but not YFP expression in a dorsal view of the pelvic ganglia from the urogenital tract shown in D–D′. Abbreviations: b, bladder; dc, distal colon; PG, pelvic ganglion; pu, pelvic urethra; pc, proximal colon.

ENPs in mutant embryos that was more severe at caudal levels of the GI tract, and suggested a role for Foxd3 in maintaining vagal NC-derived ENPs during ENS development.

Patterning and distribution, but not differentiation, of enteric neurons is disrupted in Foxd3 mutant ENS

Our previous work demonstrated that Foxd3 preserves neural potency of early NC cells (Mundell and Labosky, 2011). However, it was unknown whether Foxd3 maintains neural potency after cells are specified as ENPs. The decrease in the number of *Foxd3* mutant cells within the GI tract of *Foxd3*$^{flox/-}$*; Ednrb-iCre* embryos may indicate a similar role for Foxd3 in maintenance of neural fate of ENPs. Wholemount immunohistochemistry with subsequent confocal analysis of GI tracts from control embryos revealed a dense meshwork of tightly packed PGP9.5-positive neurons present in the duodenum (Fig. 9A). PGP9.5-expressing cells showed extensive but not complete overlap with YFP expression, suggesting that the majority of vagal NC-derived enteric neurons arise from *Ednrb-iCre*-expressing cells (Fig. 9A). In stark contrast, reduced numbers of YFP-expressing cells in duodena from *Foxd3* mutant embryos was associated with alterations in the density and distribution of enteric neurons (Fig. 9A). Similar results were seen in colons

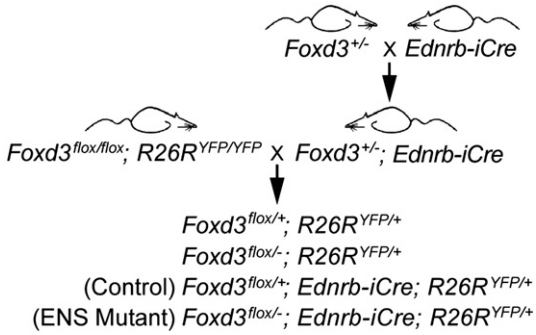

Fig. 6. Breeding strategy to generate mice with an ENS-specific deletion of *Foxd3*. Fate mapping was performed using either the $R26R^{YFP}$ allele or $R26R^{lacZ}$ allele to label *Ednrb-iCre* lineage cells in control and mutant embryos and mice.

from control and mutant embryos (Fig. 9A). Interestingly, despite a 48% reduction of YFP-positive cells in the duodenum and a 72% reduction in the colon (Fig. 9B), the majority of mutant YFP-positive cells showed co-labeling with PGP9.5, suggesting that neuronal differentiation was not overtly impaired by loss of Foxd3. This is perhaps not surprising, considering the restriction of Foxd3 expression from differentiating neurons in control GI tracts described above (Fig. 2), although these results support a different role for Foxd3 in ENPs versus early multipotent NC. To examine the density of neurons along the length of the colon we used immunodetection of PGP9.5 in sequential non-overlapping fields of colons from control and mutant embryos at 15.5 dpc (Fig. 9C). Quantification of these data clearly showed that the density of neurons was slightly decreased the whole length of the colon, but this difference was statistically significant only at the most distal end (Fig. 9D). Therefore, while Foxd3 was not absolutely required for neural differentiation, the number of ENS-neurons was greatly reduced in *Foxd3* mutant ENS.

ENPs require Foxd3 for proper glial cell differentiation and/or maintenance

Our data demonstrated that Foxd3 was initially expressed in ENPs and that expression was selectively maintained in differentiated glia during late ENS development, suggesting lineage-specific roles for Foxd3. As shown above, differentiation of neurons was not overtly impaired in mutant GI tracts. To investigate differentiation of glial lineages, we examined expression of glial markers (S100b and Sox10) in *Foxd3* mutant embryos and mice. At 16.5 dpc, analysis of S100b expression in the duodena of lineage-traced embryos revealed that, in contrast to control embryos (Fig. 10A–A″), there were reduced numbers of enteric glia from the *Ednrb-iCre* lineage in mutant guts (Fig. 10B–B″). At this stage, glial differentiation is not complete in the distal GI tract, therefore further analysis of glial differentiation

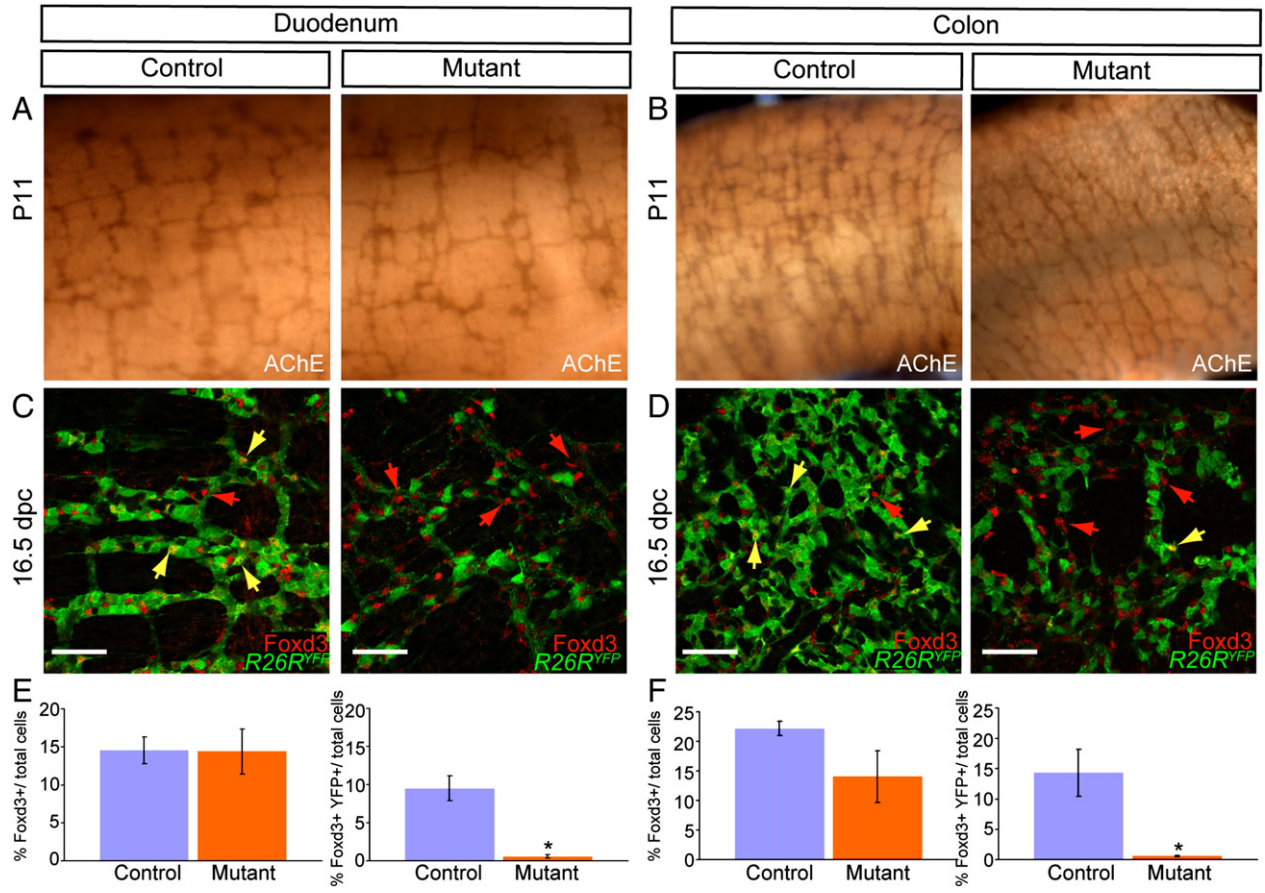

Fig. 7. Effect of deleting *Foxd3* in ENPs using *Ednrb-iCre*. (A–B) Wholemount acetylcholinesterase (AChE) histochemical staining of postnatal day 11 GI tracts revealed enteric ganglia in the duodenum (A) and colon (B) from both $Foxd3^{flox/+}$; *Ednrb-iCre* (control, left panels) and $Foxd3^{flox/-}$; *Ednrb-iCre* (mutant, right panels) mice. (C–D) In control embryonic duodenum and colon at 16.5 dpc, Foxd3 was detected in both YFP-positive *Ednrb-iCre* expressing cells (yellow nuclei, indicated with yellow arrows) and in a smaller population of YFP-negative cells (red nuclei, indicated with red arrows) (C–D, left panels). In mutant embryos, Foxd3 expression was not detected in the majority of YFP-expressing cells (C–D, right panels). However, Foxd3 expression (red) was not reduced in the duodenum (C) or distal colon (D), despite severe reduction in the number of *Ednrb-iCre*-expressing (YFP+) cells (C, D), suggesting that a subpopulation of Foxd3-expressing ENPs that does not activate *Ednrb-iCre* expression compensated for the loss of ENPs in the distal colon. (E–F) Quantification of Foxd3-expressing cells in the duodenum (graphs in E) and colon (graphs in F) from 16.5 dpc control and mutant embryos. Data represent confocal analysis of 3 (duodenum) or 6 (colon) non-overlapping adjacent fields from 3 mutant and 3 littermate control embryos. Data are portrayed as either %Foxd3+ cells or Foxd3, YFP double+ cells/DAPI+ nuclei. All statistics are mean ± SEM, *($p<0.05$) comparing control to mutant. Scale bars = 50 μm.

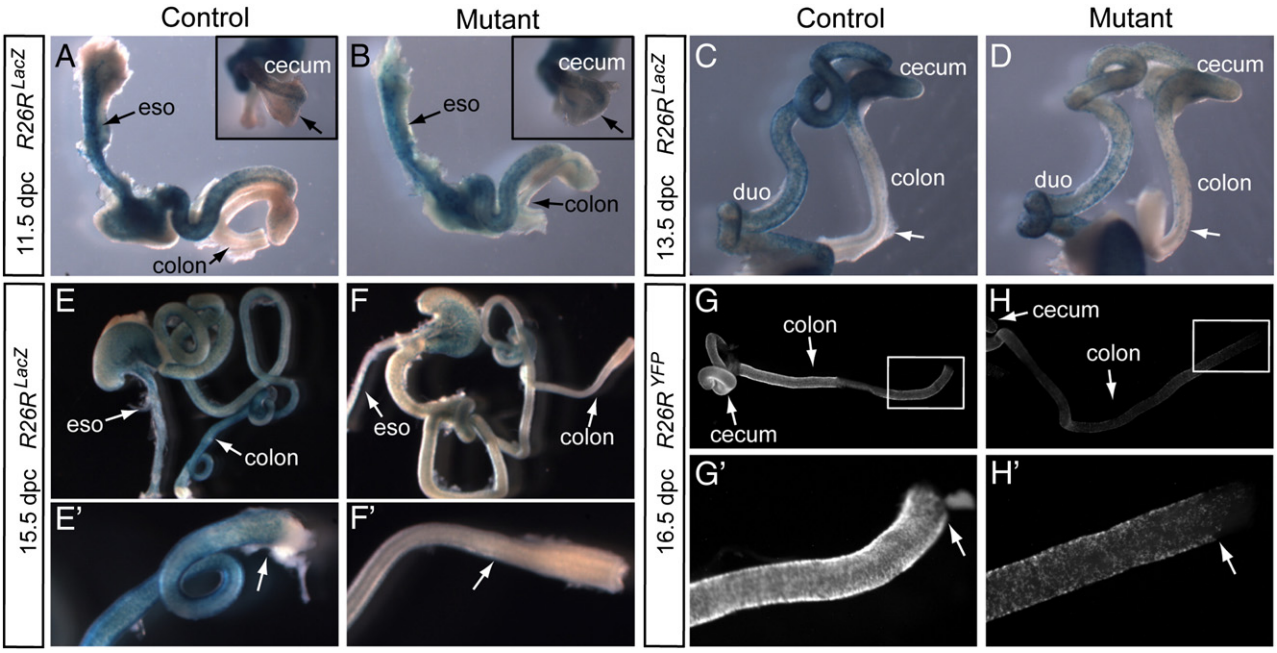

Fig. 8. Numbers of *Ednrb-iCre*-expressing ENPs were severely reduced in GI tracts from *Foxd3* mutant embryos. (A–F′) All samples shown were stained for beta-galactosidase activity from the recombined $R26R^{lacZ}$ allele (blue). Lineage labeling in control $Foxd3^{flox/+}$; *Ednrb-iCre;* $R26R^{lacZ}$ (A, C, E) and $Foxd3^{flox/-}$; *Ednrb-iCre;* $R26R^{lacZ}$ mutant embryos (B, D, F) demonstrated that the density of *Foxd3* mutant Cre-expressing cells was progressively reduced along the proximal-distal extent of the GI tract from 11.5 to 15.5 dpc. At 11.5 dpc, control ENPs populated the GI tract to the level of the cecum (A, inset arrow), and were located in the proximal colon at 13.5 dpc (C, arrow indicates caudal-most cells). At both 11.5 and 13.5 dpc, fewer *Foxd3* mutant *Ednrb-iCre* lineage cells migrated to a similar caudal level in the GI tract compared to control embryos (arrows in inset for A, B, arrows in C, D). In control embryos, X-gal-positive cells colonized the distal colon at 15.5 dpc (E, E′). *Foxd3* mutant ENPs were reduced in number throughout the GI tract and were not detected in the distal colon (F, F′). Arrows in E′ and F′ indicate caudal extent of X-gal-positive cell colonization in the distal colon. (G) Immunodetection of YFP from the recombined $R26R^{YFP}$ allele in control (G–G′) and mutant (H–H′) embryos showed that *Ednrb-iCre* expressing cells were reduced in number throughout colons from 16.5 dpc mutant embryos, but were present at the distal colon. Abbreviations: duo, duodenum; eso, esophagus.

in the colon was completed in adult ENS. Co-labeling of Sox10 with YFP in gut muscle preparations from the duodena and distal colons of adult (2–3 months old) control and mutant mice showed that, the number of Sox10/YFP double-positive cells was reduced in both duodena (Fig. 10C, D) and colons (data not shown) from mutant mice compared to controls. Quantification of enteric glia (labeled by S100b expression) and YFP-expressing cells in the duodenum and colon confirmed severely reduced numbers of differentiated glia in mutant *Ednrb-iCre* lineage cells compared to controls (Fig. 10E–H): S100b/YFP double-positive cells were reduced by 78% in duodenum (Fig. 10G) and 84% in the colon (Fig. 10H). Despite these greatly reduced numbers of glia from the *Ednrb-iCre* lineage in mutants, the overall numbers of Sox10 or S100b-positive glia were similar to controls (Fig. 10C–F), and Sox10-positive glia were present in the distal end of the colon (Fig. 9C), consistent with our hypothesis that an independent population of ENPs compensated for the loss of the Ednrb-iCre-expressing cells.

Foxd3 is required cell autonomously for proliferation of ENPs

During colonization of the GI tract, vagal ENPs proliferate in order to generate the progenitor pool needed to complete population of the entire the gut (Simpson et al., 2007). The severe reduction of *Ednrb-iCre* lineage cells we observed in mutant embryos may reflect a requirement for Foxd3 in proliferation and/or survival of ENPs. To investigate the possibility that Foxd3 is required for proliferation and expansion of the ENP pool, we monitored proliferation in the duodena and colons from $R26R^{YFP}$ fate-mapped control and mutant embryos using immunohistochemistry for phospho-histone H3 (pH3), to label cells undergoing mitosis (Fig. 11A, D). In confocal images through the developing enteric plexus, all YFP-positive cells were scored as either pH3-positive or -negative and proliferation of ENPs was calculated as the percent of *Ednrb-iCre* lineage cells (YFP+) that were also pH3-positive. Additionally, to compare proliferation of the entire ENP pool with proliferation of *Ednrb-iCre* lineage cells, we quantified the number of cells positive for both pH3 and the ENP marker Sox10 (Fig. 11A, C, D, F) in both duodena and colons (magenta arrows in Fig. 11A, D). At 14.5 dpc, proliferation of mutant YFP-positive cells in the duodena and colon was significantly reduced compared to control embryos (Fig. 11A, B, D, E). However, the overall proliferation of Sox10-expressing ENPs was unchanged in both the duodena and colons (quantified in Fig. 11C, F). This suggests that in mutants, ENPs outside the *Ednrb-iCre* lineage compensate for the loss of Foxd3 in the *Ednrb-iCre* lineage by increasing proliferation compared to control embryos. These results support the hypothesis that a sub-population of the ENS undergoes expansion to compensate for the loss of Cre-expressing *Foxd3* mutant cells. Further analysis was done to examine apoptosis in GI tracts from fate-mapped control and mutant embryos, and these experiments showed no difference between controls and mutants (data not shown), suggesting that loss of Foxd3 did not affect survival of ENPs. Together, our data demonstrate that Foxd3 is required to maintain proliferation of vagal NC-derived ENPs throughout the GI tract and suggests that deletion of Foxd3 in a subset of the ENS resulted in the compensatory proliferation of non-*Ednrb-iCre* ENS cells.

Discussion

Foxd3 is required at multiple stages of ENS development

During migration, ENPs undergo self-renewing divisions to maintain both neural and glial potency and generate a progenitor pool sufficient to form the entire ENS (Natarajan et al., 1999). Our previous work demonstrated that Foxd3 is essential in early NC progenitors for multipotency, self-renewal and generation of NC cells competent to enter the GI tract (Mundell and Labosky, 2011; Teng et al., 2008). However, the role of Foxd3 in later ENS development had not been

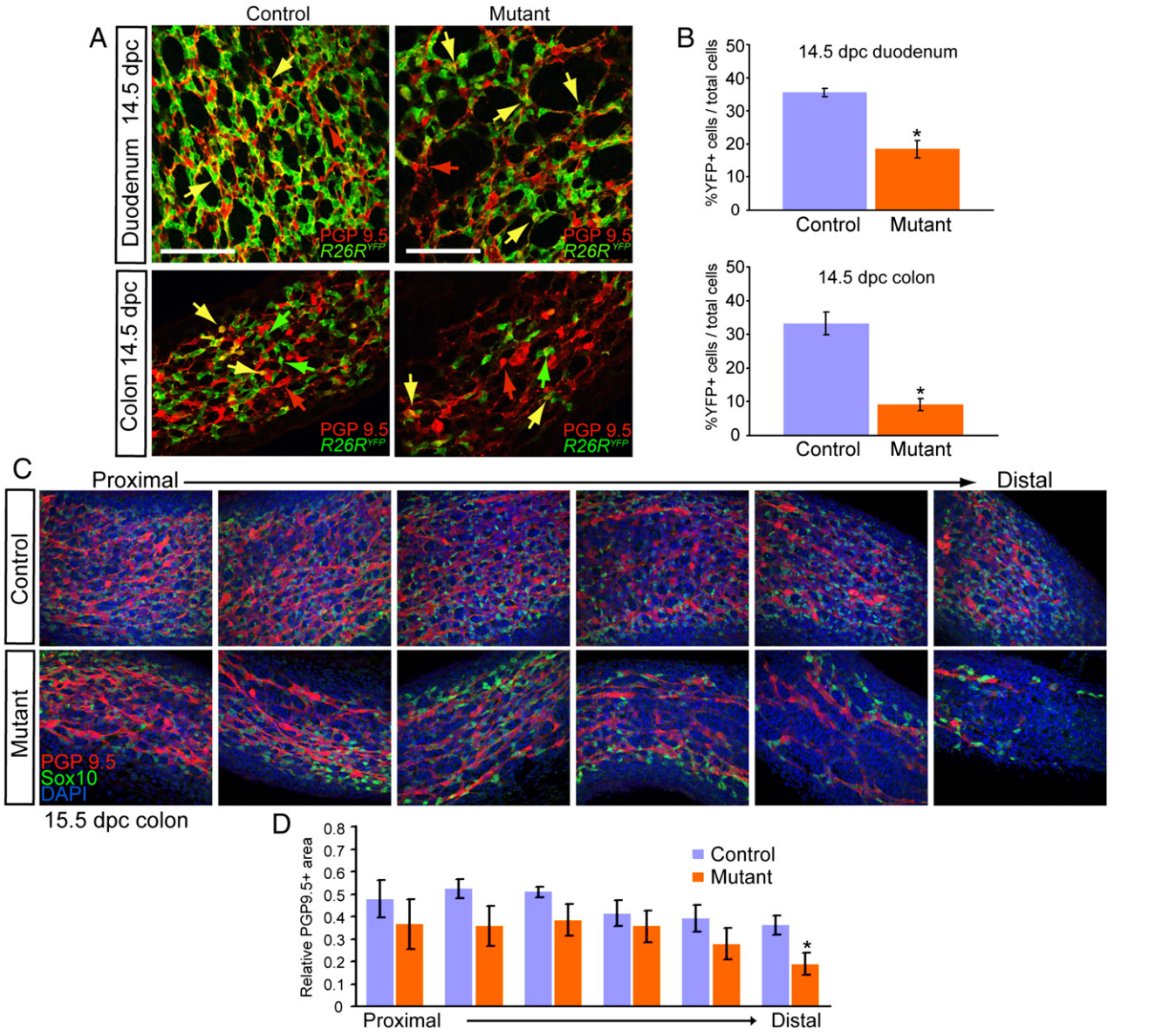

Fig. 9. Foxd3 is required for patterning and distribution but not differentiation of enteric neurons. (A–B) Characterization of neuronal differentiation in *Endrb-iCre; R26R*^{YFP} fate mapped control and *Foxd3* mutant GI tracts. Confocal images of wholemount immunohistochemistry for YFP (green) and PGP9.5 (red) identified two populations of enteric neurons in control embryos: *Ednrb-iCre* derived neurons (yellow arrows in A) and a relatively smaller population of neurons that did not show Cre activity (red arrows). Both *Ednrb-iCre* derived and YFP-negative neurons organized into a regular meshwork pattern of developing ganglia in the duodena from 14.5 dpc control embryos (A). In *Foxd3* mutant embryos, ENS patterning was dramatically disrupted and included areas of thin projections from fewer enteric neurons. In GI tracts from mutant embryos, YFP-positive cells showed extensive overlap with PGP9.5 (yellow arrows), but the majority of enteric neurons do not show *Ednrb-iCre* activity (red arrows). (B) Quantification of YFP-expressing cells in duodena and colons from 14.5 dpc control and mutant embryos. Data represent confocal analysis of 3 non-overlapping adjacent fields from the duodenum and 6 fields from the colon from 3 mutant and 3 littermate control embryos. Data are portrayed as %YFP + cells / DAPI + nuclei. All statistics are mean ± SEM, *($p<0.05$) comparing control to mutant. (C) Expression of PGP9.5 (red, neurons), Sox10 (green, ENPs and glia) and DAPI (Blue) in 6 sequential, non-overlapping fields of the colon from control (top) and mutant (bottom) embryos showed numbers of PGP9.5 + neurons and Sox10 + cells progressively decreased in proximal-to-distal regions of the colon. (D) Quantification of the density of PGP9.5-expressing neurons (PGP9.5 + pixel area / total pixel area) in 6 sequential 40× fields from colons of 14.5 dpc control and mutant embryos. Data represent confocal analysis of fields that show the highest PGP9.5 + area in z stacks for 6 distinct proximal-to-distal regions of the colon from 4 mutant and 4 littermate control embryos. All statistics are mean ± SEM, *($p<0.05$) comparing control to mutant. Scale bars = 100 μm.

examined. Here, we present data demonstrating that Foxd3 expression is maintained in both ENPs and glia and that Foxd3 plays a critical role in ENPs and glia throughout development of the ENS. Further, we identify a subpopulation of Foxd3-expressing ENPs that undergo regulative proliferation and differentiation to compensate for loss of a large portion of the ENPs that express *Ednrb-iCre*.

Activity of Ednrb-iCre is specific for vagal NC cells

We generated and characterized an ENS-specific transgenic Cre line that labels vagal, but not sacral-derived, ENPs. *Ednrb-iCre* activity is first detected in vagal-derived NC cells at 11.0 dpc as ENPs migrate through the midgut and cecum. Using molecular markers in combination with fate mapping of the *Ednrb-iCre* lineage, we demonstrated that this novel *Ednrb-iCre* transgene labels the majority of Foxd3-expressing cells within vagal-derived ENPs and the *Ednrb-iCre* lineage cells generate both neurons and glia during ENS development. Our finding that *Ednrb-iCre* expression specifically labels vagal, but not sacral NC, suggests that this novel Cre transgene could be useful for identification of molecular differences between vagal and sacral NC cells during development. Previous studies suggested that vagal and sacral NC have intrinsic differences in their ability to generate the ENS (Burns et al., 2002; Burns and Le Douarin, 1998). However, there is considerable controversy about the relative role of sacral versus vagal NC, primarily due

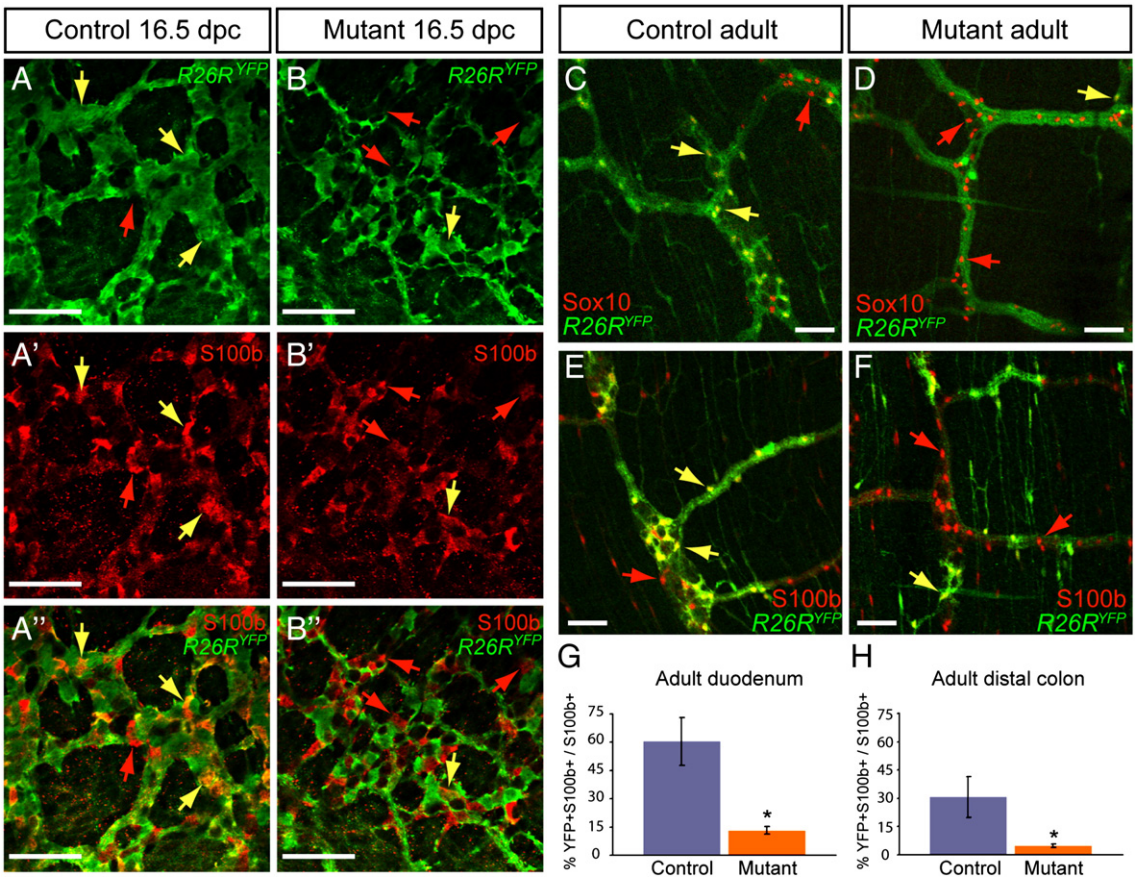

Fig. 10. Analysis of glial differentiation during ENS development in mutant and control embryos and mice. (A–B″) YFP (*Ednrb-iCre* activity, green) and S100b (glia, red) expression in control (A–A″) and *Foxd3* mutant (B-B″) duodena at 16.5 dpc. Co-localization of S100b and YFP (yellow arrows) was diminished in mutant ENS. Red arrows indicate glia that did not express YFP. (C–D) Immunodetection of YFP (green) with Sox10 expression (glia, red) in the duodena from adult control (C) and *Foxd3* mutant (D) mice showed reduced numbers of glia derived from the *Ednrb-iCre* lineage. Yellow arrows indicate co-expression of Sox10 and YFP. (E–H) S100b/YFP double-positive enteric glia (yellow arrows) were depleted in the mature ENS from mutant mice (E) compared to controls (F). Data in G and H represent 3 independent experiments in which S100b-positive glial cells were counted in random fields from the duodenum (n = 3 control and 5 mutant mice) and the colon (n = 3 control and 4 mutant mice). Scale bars = 50 μm. All statistics are mean ± SEM, *($p<0.05$).

to lack of specific molecular markers for each population. Gene profiling of vagal versus sacral NC from neural tube explant cultures failed to identify genes specifically expressed in either NC population (Delalande et al., 2008), suggesting that identification of migratory vagal and sacral ENPs in situ may be required to definitively profile their gene expression and in vivo characteristics. Although there are a few molecular markers limited in their expression to the vagal NC, including *a Hoxb3* enhancer, which is expressed in a sub-population of vagal NC-derived neurons but absent from enteric glial lineages (Chan et al., 2005; Lui et al., 2008), a specific and all-encompassing marker of vagal NC cells remains elusive. Currently, the relative extent of sacral NC contribution to the distal GI tract in mammals as well as intrinsic molecular differences between these two NC populations is unknown. Our data suggest that lineage labeling of *Ednrb-iCre* expressing cells would allow for prospective isolation and gene profiling of the overwhelming majority of vagal NC-derived cells from the GI tract, potentially resolving some of these unanswered questions.

Maintenance of proliferation and gliogenesis during ENS development

Foxd3 is broadly expressed as ENPs enter the gut and then downregulated as they undergo progressive differentiation to neuronal fates. In contrast, Foxd3 was maintained in p75-expressing ENPs and S100b-positive glia well after initial ENP colonization of the GI tract. Our data demonstrating that Foxd3 is required to maintain proliferation and glial differentiation, but not neuronal differentiation, are consistent with the temporal expression of Foxd3. This is also consistent with the possibility that downregulation of Foxd3 in ENPs may be an important step in specification of enteric neurons. This is in contrast to recent data showing that the transcription factor Hand2 functions primarily in neurogenesis (Lei and Howard, 2011), implying molecularly distinct programs of differentiation for these two co-dependent lineages. At present, the transcription factors and signaling pathways that regulate the dynamic expression of Foxd3 during ENS development are unknown and the molecular pathways in which Foxd3 functions to maintain both ENPs and enteric glia have not yet been identified.

Examination of the spatiotemporal expression pattern of Foxd3 revealed that it is comparable to Sox10 expression during ENS development (Kuhlbrodt et al., 1998). Here we showed that Foxd3 is required to maintain Sox10-expressing glia within the *Ednrb-iCre* lineage, consistent with our previous work in other regions of the NC (Mundell and Labosky, 2011; Teng et al., 2008). Because Sox10 is essential for the maintenance of ENPs (Paratore et al., 2002; Southard-Smith et al., 1998), and for differentiation and maturation of peripheral nervous system glia (Britsch et al., 2001; Finzsch et al., 2010), it is possible that the combined defects in maintenance of ENPs and specification of enteric glia observed in *Foxd3$^{flox/-}$; Ednrb-iCre* embryos may be related to loss or reduction of Sox10. At present there is no genetic evidence of a functional interaction between Foxd3 and Sox10, although bioinformatic analysis identified putative Foxd3 binding sites in the first intron of the zebrafish *sox10* gene, (Dutton et al., 2008) and more recent work described a different Foxd3 binding site upstream of *Sox10* and a synergistic mechanism

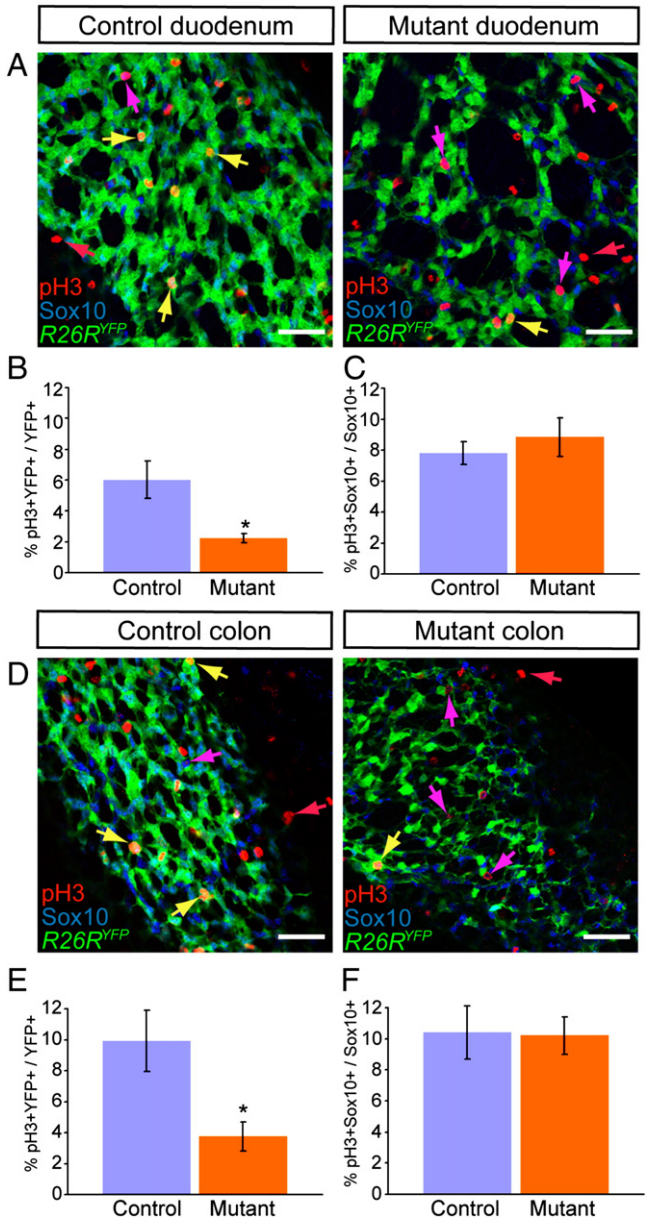

Fig. 11. Foxd3 is required for proliferation of ENPs. (A–C) Immunofluorescence for pH3 (cells undergoing mitosis), Sox10 (ENPs and glia) and YFP (*Endrb-iCre* lineage) in duodena from 14.5 dpc control (A, left panel) and *Foxd3* mutant (A, right panel) embryos carrying the $R26R^{YFP}$ allele. Yellow arrows indicate YFP and pH3 double-positive cells. Magenta arrows indicate pH3-positive, Sox10-expressing cells that did not co-express YFP. Red arrows indicate cells that are pH3-positive but YFP- and Sox10-negative, presumably mesenchymal cells. Quantification of the percent of proliferating *Ednrb*-iCre-lineage cells in the duodena is shown in B and the percent of proliferating Sox10+ cells is shown in C. Despite a clear reduction in the percent of proliferating YFP-positive cells in mutant embryos compared to controls (A, B), the total level of ENP cell proliferation in the duodena was unchanged in mutant embryos (C). (D–F) Immunofluorescence for YFP, Sox10 and pH3 in colons from control and mutant embryos showed decreased proliferation of *Ednrb-iCre* lineage cells in mutants (D). Quantification of the proliferating *Ednrb-iCre* lineage cells (E) and the proliferation of Sox10-positive cells (F) in colons from 14.5 dpc control and mutant embryos again showed a decrease in proliferation in YFP-positive *Foxd3* mutant ENPs and a subsequent increase in Sox10-expressing cells that did not co-express YFP. Data represent confocal analysis of GI tracts from 3 mutant and 3 littermate control embryos. 9 non-overlapping 40× confocal images (3 fields from duodena and 6 fields from colons) were analyzed from each embryo. *($p<0.05$). Scale bars = 50 μm. All statistics are mean ± SEM, *($p<0.05$).

between Foxd3 and Sox2 proteins in the control of *Sox10* transcription in murine NC-derived neuroblastoma cell lines (Wahlbuhl et al., 2011). Further investigation of the precise pathways and mechanisms through which Foxd3 maintains ENS proliferation and gliogenesis will provide a more complete understanding of the transcriptional regulation mediating ENS development.

Compensation in Foxd3 mutant ENS

A surprising finding from our work is that deletion of *Foxd3* in the *Ednrb-iCre* lineage does not disturb the overt function of the ENS; the mutant mice appear healthy and we detected no changes in weight or lifespan. Despite initial disruption of neural patterning at embryonic stages, AChE histochemistry revealed only modest alterations in connectivity of postnatal enteric ganglia, and lethality or obstructive bowel disease was not evident in postnatal or adult mutant mice. Our lineage-mapping data demonstrate that normally, ENPs within the *Ednrb-iCre* lineage contribute the majority of neurons and glia within the developing ENS. In fact, a deletion of the endogenous *Ednrb* ENS-specific enhancer used to generate the *Ednrb-iCre* transgene resulted in loss of ENPs in the cecum and hindgut and postnatal death from megacolon (Zhu et al., 2004). This clearly demonstrates that the ENPs activating this enhancer are critical for late stages of ENS development. In contrast, in *Foxd3* mutants, we describe a profound shift in the relative contribution of enteric sub-lineages such that the ENS was primarily formed from non-*Ednrb-iCre* lineage cells. Our results are consistent with the possibility that an independent population of ENPs expands in number following deletion of Foxd3 within the *Ednrb-iCre* lineage. Concomitant with decreased proliferation in mutant *Ednrb-iCre*-expressing cells, overall proliferation in the ENP pool was unchanged compared to controls. We interpret these data to conclude that a unique sub-population of Foxd3 and Sox10-expressing ENPs that did not express the *Ednrb-iCre* transgene underwent activation, regulative proliferation and differentiation into both neuronal and glial lineages in response to the severe depletion of *Ednrb-iCre* lineage cells.

Regulative lineage compensation, in which an independent cell population functionally compensates for loss of another, may be a common mechanism for overcoming developmental deficiencies. However, few studies have defined mammalian cell populations with this potential. During skeletal muscle development in mice, conditional ablation of Myf5-expressing cells results in lineage compensation by a Myf5-independent cell population that prevents disruption of myogenesis (Haldar et al., 2008). In the zebrafish NC, regulative lineage compensation has been suggested for genetically distinct populations of NC-derived melanophore precursors; depletion of *erbb3b*-dependent nerve-associated melanophore precursors resulted in increased proliferation and differentiation of remaining melanophore progenitors (Budi et al., 2011). This is not the first description of compensation within the ENS; a deletion of Hand2 in the Nestin-expressing ENPs resulted in compensation from ENPs that did not express the *Nestin-Cre* transgene used in that study (Lei and Howard, 2011). In addition, the compensatory changes we observe here are similar to those observed in chimeric mice showing that a lack of *Ednrb* in a sub population of ENPs could be overcome by wild type ENPs in the duodenum but not in the distal colon (Kapur et al., 1995). An alternative possibility is that the *Ednrb-iCre* lineage may represent a more restricted transient-amplifying ENP population able to generate some neural and glial cells, but distinct from multipotent NCSCs present during initial colonization of the GI tract. While our data suggest the ENS in $Foxd3^{flox/-}$; *Ednrb-iCre* mice contained neurons and glia that were quantitatively comparable to control mice, we cannot rule out the possibility that some enteric cell types were differently affected by the loss of Foxd3. Our data demonstrating increased non-*Ednrb-iCre* lineage proliferation and gliogenesis in both the duodenum and colon of *Foxd3* mutant embryos suggests that sacral NC may not compensate for loss of *Ednrb-iCre* lineage cells in all regions of the GI tract. However, given that Foxd3 was deleted after vagal NC colonization of the proximal GI tract,

another possibility is that the sacral NC ENP pool was activated to form an increased proportion of the distal ENS.

Implications for regenerative medicine

NCSC replacement has been suggested as a cell-based therapy for Hirschsprung's disease and other GI neurodegenerative diseases (Bondurand et al., 2003; Kruger et al., 2002; Micci and Pasricha, 2007). However, therapeutic use of NCSCs for regeneration of the ENS will require a better understanding of the dynamic cellular properties of ENPs and the distinct sub-populations of ENPs that generate the ENS during development. Recent data showed that adult gut-derived NCSCs, while they have the capacity to generate both neurons and glia in vitro, give rise predominantly to glia in physiological settings, thereby suggesting that ENS neurogenesis from autologous sources may be challenging (Joseph et al., 2011). The ability to activate intrinsic enteric NCSC populations to induce repair of congenital bowel defects is an intriguing possibility. However, before that possibility can be realized, it will be important to identify genes and signaling pathways controlling the self-renewal, migration and differentiation of ENPs in vivo. Our findings demonstrate several crucial roles played by Foxd3 during ENS development including maintenance of the ENP pool, neural patterning and glial differentiation. In addition, our results suggest that distinct sub-lineages of ENPs are intrinsically able to respond to ENS injury or disease.

Supplementary materials related to this article can be found online at doi:10.1016/j.ydbio.2012.01.003.

Acknowledgments

We thank Elise Pfaltzgraff for assistance with immunohistochemistry, Alexander Nickle for AChE histochemistry, Jason Kappa and Leshana Saint-Jean for preliminary analysis of enteric glia, and Dr. Mark Magnuson for use of microscopes. Olympus FV1000 confocal microscopy was performed in part through use of the VUMC Cell Imaging Shared Resource (supported by NIH grants CA68485, DK20593, DK58404, HD15052, DK59637 and EY08126). This work was supported by grants from the NIH (HD36720 and HD036720-11S109) to PAL, predoctoral fellowships from the American Heart Association (0615209B) and NIH (NS065604) to NAM, a predoctoral fellowship from the American Heart Association to JLP (10PRE4500024), NIH (DK60047) and a March of Dimes Award 1-FY06-390 to MS^2 and Vanderbilt University Medical Center Academic Program Support.

References

Abramoff, M.D., Magelhaes, P.J., Ram, S.J., 2004. Image processing with image. J. Biophotonics Int. 11, 36–42.
Baetge, G., Gershon, M.D., 1989. Transient catecholaminergic (TC) cells in the vagus nerves and bowel of fetal mice: relationship to the development of enteric neurons. Dev. Biol. 132, 189–211.
Barlow, A., de Graaff, E., Pachnis, V., 2003. Enteric nervous system progenitors are coordinately controlled by the G protein-coupled receptor EDNRB and the receptor tyrosine kinase RET. Neuron 40, 905–916.
Baynash, A.G., Hosoda, K., Giaid, A., Richardson, J.A., Emoto, N., Hammer, R.E., Yanagisawa, M., 1994. Interaction of endothelin-3 with endothelin-B receptor is essential for development of epidermal melanocytes and enteric neurons. Cell 79, 1277–1285.
Bondurand, N., Natarajan, D., Barlow, A., Thapar, N., Pachnis, V., 2006. Maintenance of mammalian enteric nervous system progenitors by SOX10 and endothelin 3 signalling. Development 133, 2075–2086.
Bondurand, N., Natarajan, D., Thapar, N., Atkins, C., Pachnis, V., 2003. Neuron and glia generating progenitors of the mammalian enteric nervous system isolated from foetal and postnatal gut cultures. Development 130, 6387–6400.
Britsch, S., Goerich, D.E., Riethmacher, D., Peirano, R.I., Rossner, M., Nave, K.A., Birchmeier, C., Wegner, M., 2001. The transcription factor Sox10 is a key regulator of peripheral glial development. Genes Dev. 15, 66–78.
Budi, E.H., Patterson, L.B., Parichy, D.M., 2011. Post-embryonic nerve-associated precursors to adult pigment cells: genetic requirements and dynamics of morphogenesis and differentiation. PLoS Genet. 7, e1002044.
Burns, A.J., Champeval, D., Le Douarin, N.M., 2000. Sacral neural crest cells colonise aganglionic hindgut in vivo but fail to compensate for lack of enteric ganglia. Dev. Biol. 219, 30–43.
Burns, A.J., Delalande, J.M., Le Douarin, N.M., 2002. In ovo transplantation of enteric nervous system precursors from vagal to sacral neural crest results in extensive hindgut colonisation. Development 129, 2785–2796.
Burns, A.J., Le Douarin, N.M., 1998. The sacral neural crest contributes neurons and glia to the post-umbilical gut: spatiotemporal analysis of the development of the enteric nervous system. Development 125, 4335–4347.
Cantrell, V.A., Owens, S.E., Chandler, R.L., Airey, D.C., Bradley, K.M., Smith, J.R., Southard-Smith, E.M., 2004. Interactions between Sox10 and EdnrB modulate penetrance and severity of aganglionosis in the Sox10Dom mouse model of Hirschsprung disease. Hum. Mol. Genet. 13, 2289–2301.
Chan, K.K., Chen, Y.S., Yau, T.O., Fu, M., Lui, V.C., Tam, P.K., Sham, M.H., 2005. Hoxb3 vagal neural crest-specific enhancer element for controlling enteric nervous system development. Dev. Dyn. 233, 473–483.
Corpening, J.C., Cantrell, V.A., Deal, K.K., Southard-Smith, E.M., 2008. A Histone2BCerulean BAC transgene identifies differential expression of Phox2b in migrating enteric neural crest derivatives and enteric glia. Dev. Dyn. 237, 1119–1132.
Corpening, J.C., Deal, K.K., Cantrell, V.A., Skelton, S.B., Buehler, D.P., Southard-Smith, E.M., 2011. Isolation and live imaging of enteric progenitors based on Sox10-histone2bvenus transgene expression. Genesis 49, 599–618.
Danielian, P.S., Muccino, D., Rowitch, D.H., Michael, S.K., McMahon, A.P., 1998. Modification of gene activity in mouse embryos in utero by a tamoxifen-inducible form of Cre recombinase. Curr. Biol. 8, 1323–1326.
Deal, K.K., Cantrell, V.A., Chandler, R.L., Saunders, T.L., Mortlock, D.P., Southard-Smith, E.M., 2006. Distant regulatory elements in a Sox10-beta GEO BAC transgene are required for expression of Sox10 in the enteric nervous system and other neural crest-derived tissues. Dev. Dyn. 235, 1413–1432.
Delalande, J.M., Barlow, A.J., Thomas, A.J., Wallace, A.S., Thapar, N., Erickson, C.A., Burns, A.J., 2008. The receptor tyrosine kinase RET regulates hindgut colonization by sacral neural crest cells. Dev. Biol. 313, 279–292.
Druckenbrod, N.R., Epstein, M.L., 2005. The pattern of neural crest advance in the cecum and colon. Dev. Biol. 287, 125–133.
Dutton, J.R., Antonellis, A., Carney, T.J., Rodrigues, F.S., Pavan, W.J., Ward, A., Kelsh, R.N., 2008. An evolutionarily conserved intronic region controls the spatiotemporal expression of the transcription factor Sox10. BMC Dev. Biol. 8, 105.
Enomoto, H., Araki, T., Jackman, A., Heuckeroth, R.O., Snider, W.D., Johnson Jr., E.M., Milbrandt, J., 1998. GFR alpha1-deficient mice have deficits in the enteric nervous system and kidneys. Neuron 21, 317–324.
Finzsch, M., Schreiner, S., Kichko, T., Reeh, P., Tamm, E.R., Bosl, M.R., Meijer, D., Wegner, M., 2010. Sox10 is required for Schwann cell identity and progression beyond the immature Schwann cell stage. J. Cell Biol. 189, 701–712.
Gershon, M.D., 2010. Developmental determinants of the independence and complexity of the enteric nervous system. Trends Neurosci. 33, 446–456.
Gershon, M.D., Chalazonitis, A., Rothman, T.P., 1993. From neural crest to bowel: development of the enteric nervous system. J. Neurobiol. 24, 199–214.
Haldar, M., Karan, G., Tvrdik, P., Capecchi, M.R., 2008. Two cell lineages, myf5 and myf5-independent, participate in mouse skeletal myogenesis. Dev. Cell 14, 437–445.
Hanna, L.A., Foreman, R.K., Tarasenko, I.A., Kessler, D.S., Labosky, P.A., 2002. Requirement for Foxd3 in maintaining pluripotent cells of the early mouse embryo. Genes Dev. 16, 2650–2661.
Heanue, T.A., Pachnis, V., 2007. Enteric nervous system development and Hirschsprung's disease: advances in genetic and stem cell studies. Nat. Rev. Neurosci. 8, 466–479.
Hearn, C.J., Murphy, M., Newgreen, D., 1998. GDNF and ET-3 differentially modulate the numbers of avian enteric neural crest cells and enteric neurons in vitro. Dev. Biol. 197, 93–105.
Hosoda, K., Hammer, R.E., Richardson, J.A., Baynash, A.G., Cheung, J.C., Giaid, A., Yanagisawa, M., 1994. Targeted and natural (piebald-lethal) mutations of endothelin-B receptor gene produce megacolon associated with spotted coat color in mice. Cell 79, 1267–1276.
Iwashita, T., Kruger, G.M., Pardal, R., Kiel, M.J., Morrison, S.J., 2003. Hirschsprung disease is linked to defects in neural crest stem cell function. Science 301, 972–976.
Joseph, N.M., He, S., Quintana, E., Kim, Y.G., Nunez, G., Morrison, S.J., 2011. Enteric glia are multipotent in culture but primarily form glia in the adult rodent gut. J. Clin. Invest. 121, 3398–3411.
Kapur, R.P., 2000. Colonization of the murine hindgut by sacral crest-derived neural precursors: experimental support for an evolutionarily conserved model. Dev. Biol. 227, 146–155.
Kapur, R.P., Sweetser, D.A., Doggett, B., Siebert, J.R., Palmiter, R.D., 1995. Intercellular signals downstream of endothelin receptor-B mediate colonization of the large intestine by enteric neuroblasts. Development 121, 3787–3795.
Kim, J., Lo, L., Dormand, E., Anderson, D.J., 2003. SOX10 maintains multipotency and inhibits neuronal differentiation of neural crest stem cells. Neuron 38, 17–31.
Kruger, G.M., Mosher, J.T., Bixby, S., Joseph, N., Iwashita, T., Morrison, S.J., 2002. Neural crest stem cells persist in the adult gut but undergo changes in self-renewal, neuronal subtype potential, and factor responsiveness. Neuron 35, 657–669.
Kruger, G.M., Mosher, J.T., Tsai, Y.H., Yeager, K.J., Iwashita, T., Gariepy, C.E., Morrison, S.J., 2003. Temporally distinct requirements for endothelin receptor B in the generation and migration of gut neural crest stem cells. Neuron 40, 917–929.
Kuhlbrodt, K., Herbarth, B., Sock, E., Hermans-Borgmeyer, I., Wegner, M., 1998. Sox10, a novel transcriptional modulator in glial cells. J. Neurosci. 18, 237–250.
Labosky, P.A., Kaestner, K.H., 1998. The winged helix transcription factor Hfh2 is expressed in neural crest and spinal cord during mouse development. Mech. Dev. 76, 185–190.
Le Douarin, N.M., Kalcheim, C., 1999. The Neural Crest, Second Edition. Cambridge University Press, Cambridge.

Le Douarin, N.M., Teillet, M.A., 1973. The migration of neural crest cells to the wall of the digestive tract in avian embryo. J. Embryol. Exp. Morphol. 30, 31–48.
Lee, H.O., Levorse, J.M., Shin, M.K., 2003. The endothelin receptor-B is required for the migration of neural crest-derived melanocyte and enteric neuron precursors. Dev. Biol. 259, 162–175.
Lei, J., Howard, M.J., 2011. Targeted deletion of Hand2 in enteric neural precursor cells affects its functions in neurogenesis, neurotransmitter specification and gangliogenesis, causing functional aganglionosis. Development 138, 4789–4800.
Lui, V.C., Cheng, W.W., Leon, T.Y., Lau, D.K., Garcia-Barcelo, M.M., Miao, X.P., Kam, M.K., So, M.T., Chen, Y., Wall, N.A., Sham, M.H., Tam, P.K., 2008. Perturbation of hoxb5 signaling in vagal neural crests down-regulates ret leading to intestinal hypoganglionosis in mice. Gastroenterology 134, 1104–1115.
Metzger, M., Caldwell, C., Barlow, A.J., Burns, A.J., Thapar, N., 2009. Enteric nervous system stem cells derived from human gut mucosa for the treatment of aganglionic gut disorders. Gastroenterology 136 (2214–2225), e2211–e2213.
Micci, M.A., Pasricha, P.J., 2007. Neural stem cells for the treatment of disorders of the enteric nervous system: strategies and challenges. Dev. Dyn. 236, 33–43.
Mundell, N.A., Labosky, P.A., 2011. Neural crest stem cell multipotency requires Foxd3 to maintain neural potential and repress mesenchymal fates. Development 138, 641–652.
Nagy, A., Gertsenstein, M., Vintersten, K., Behringer, R., 2003. Manipulating the Mouse Embryo: A Laboratory Manual, 3 ed. Cold Spring Harbor Laboratory Press, Cold Spring Harbor, NY.
Natarajan, D., Grigoriou, M., Marcos-Gutierrez, C.V., Atkins, C., Pachnis, V., 1999. Multipotential progenitors of the mammalian enteric nervous system capable of colonising aganglionic bowel in organ culture. Development 126, 157–168.
Nelms, B.L., Pfaltzgraff, E.R., Labosky, P.A., 2011. Functional interaction between Foxd3 and Pax3 in cardiac neural crest development. Genesis 49, 10–23.
Okamura, Y., Saga, Y., 2008. Notch signaling is required for the maintenance of enteric neural crest progenitors. Development 135, 3555–3565.
Paratore, C., Eichenberger, C., Suter, U., Sommer, L., 2002. Sox10 haploinsufficiency affects maintenance of progenitor cells in a mouse model of Hirschsprung disease. Hum. Mol. Genet. 11, 3075–3085.
Pattyn, A., Morin, X., Cremer, H., Goridis, C., Brunet, J.F., 1999. The homeobox gene Phox2b is essential for the development of autonomic neural crest derivatives. Nature 399, 366–370.
Perera, H.K., Caldwell, M.E., Hayes-Patterson, D., Teng, L., Peshavaria, M., Jetton, T.L., Labosky, P.A., 2006. Expression and shifting subcellular localization of the transcription factor, Foxd3, in embryonic and adult pancreas. Gene Expr. Patterns 6, 971–977.
Plank, J.L., Mundell, N.A., Frist, A.Y., LeGrone, A.W., Kim, T., Musser, M.A., Walter, T.J., Labosky, P.A., 2011. Influence and timing of arrival of murine neural crest on pancreatic beta cell development and maturation. Dev. Biol. 349, 321–330.
Presnell, J.K., Schreibman, M.P., 1997. Humason's Animal Tissue Techniques, 5 ed. The Johns Hopkins University Press, Baltimore, MD.
Schuchardt, A., D'Agati, V., Larsson-Blomberg, L., Costantini, F., Pachnis, V., 1994. Defects in the kidney and enteric nervous system of mice lacking the tyrosine kinase receptor Ret. Nature 367, 380–383.
Shimshek, D.R., Kim, J., Hubner, M.R., Spergel, D.J., Buchholz, F., Casanova, E., Stewart, A.F., Seeburg, P.H., Sprengel, R., 2002. Codon-improved Cre recombinase (iCre) expression in the mouse. Genesis 32, 19–26.
Simpson, M.J., Zhang, D.C., Mariani, M., Landman, K.A., Newgreen, D.F., 2007. Cell proliferation drives neural crest cell invasion of the intestine. Dev. Biol. 302, 553–568.
Soriano, P., 1999. Generalized lacZ expression with the ROSA26 Cre reporter strain. Nat. Genet. 21, 70–71.
Southard-Smith, E.M., Kos, L., Pavan, W.J., 1998. Sox10 mutation disrupts neural crest development in Dom Hirschsprung mouse model. Nat. Genet. 18, 60–64.
Srinivas, S., Watanabe, T., Lin, C.S., William, C.M., Tanabe, Y., Jessell, T.M., Costantini, F., 2001. Cre reporter strains produced by targeted insertion of EYFP and ECFP into the ROSA26 locus. BMC Dev. Biol. 1, 4.
Taylor, M.K., Yeager, K., Morrison, S.J., 2007. Physiological Notch signaling promotes gliogenesis in the developing peripheral and central nervous systems. Development 134, 2435–2447.
Teng, L., Mundell, N.A., Frist, A.Y., Wang, Q., Labosky, P.A., 2008. Requirement for Foxd3 in the maintenance of neural crest progenitors. Development 135, 1615–1624.
Tompers, D.M., Foreman, R.K., Wang, Q., Kumanova, M., Labosky, P.A., 2005. Foxd3 is required in the trophoblast progenitor cell lineage of the mouse embryo. Dev. Biol. 285, 126–137.
Wahlbuhl, M., Reiprich, S., Vogl, M.R., Bosl, M.R., Wegner, M., 2011. Transcription factor Sox10 orchestrates activity of a neural crest-specific enhancer in the vicinity of its gene. Nucleic Acids Res. 40, 88–101.
Wu, J.J., Chen, J.X., Rothman, T.P., Gershon, M.D., 1999. Inhibition of in vitro enteric neuronal development by endothelin-3: mediation by endothelin B receptors. Development 126, 1161–1173.
Yntema, C.L., Hammond, W.S., 1954. The origin of intrinsic ganglia of trunk viscera from vagal neural crest in the chick embryo. J. Comp. Neurol. 101, 515–541.
Young, H.M., Bergner, A.J., Muller, T., 2003. Acquisition of neuronal and glial markers by neural crest-derived cells in the mouse intestine. J. Comp. Neurol. 456, 1–11.
Young, H.M., Ciampoli, D., Hsuan, J., Canty, A.J., 1999. Expression of Ret-, p75(NTR)-, Phox2a-, Phox2b-, and tyrosine hydroxylase-immunoreactivity by undifferentiated neural crest-derived cells and different classes of enteric neurons in the embryonic mouse gut. Dev. Dyn. 216, 137–152.
Young, H.M., Hearn, C.J., Ciampoli, D., Southwell, B.R., Brunet, J.F., Newgreen, D.F., 1998. A single rostrocaudal colonization of the rodent intestine by enteric neuron precursors is revealed by the expression of Phox2b, Ret, and p75 and by explants grown under the kidney capsule or in organ culture. Dev. Biol. 202, 67–84.
Young, H.M., Turner, K.N., Bergner, A.J., 2005. The location and phenotype of proliferating neural-crest-derived cells in the developing mouse gut. Cell Tissue Res. 320, 1–9.
Zhu, L., Lee, H.O., Jordan, C.S., Cantrell, V.A., Southard-Smith, E.M., Shin, M.K., 2004. Spatiotemporal regulation of endothelin receptor-B by SOX10 in neural crest-derived enteric neuron precursors. Nat. Genet. 36, 732–737.